

Fachhochschule Aachen

**Fachbereich
Maschinenbau und Mechatronik**

**Deutsch-französischer Studiengang Maschinenbau
Konstruktionstechnik**

**Aircraft components with uniaxial fibre-
reinforced composites**

Christoph David

Matr.-Nr.: 291238

Referent : Prof. Dr.-Ing. Raatschen

16.11.2009

**In Zusammenarbeit mit
ST3D, Toulouse-Labège (Frankreich)**

Aircraft components with uniaxial fibre-reinforced composites

18/11/09

Declaration

I assure hereby, that the following diploma thesis in its entire form was written by myself and that no other references than those listed in the bibliography were used. Quotes, which were taken word by word or in a similar sense are marked. The figures and graphics in this report are selfmade or referenced if not so. This report has not been published or shown to any examination board before.

location, date

Confidentially

This diploma thesis may not, neither completely nor in extracts, be published, replicated or referred to a third party without the written consent of the author, the mentoring referee and respectively the company ST GROUP.

Acknowledgment

First, I want to thank Prof. Dr.-Ing. Raatschen from Germany and Prof. Ph.D. Bouvet from France for supporting me during this diploma thesis and for their helpful and encouraging conversations. Furthermore, I thank Prof. Dr.-Ing. Raatschen for his very friendly and helpful mentoring during the last four years of the german and french studies.

I thank Camille Barreau for his friendly mentoring throughout the internship.

Furthermore, I would thank Christophe Briols, project manager, Alain Grillet, chief executive and Stephane Trento, director of ST GROUP.

I want to say thank you to my parents who have always helped me and thanks to my aunt Elisabeth for her special support.

Summary

This diploma thesis shows how cockpit furniture is designed, so that it is capable of supporting all stresses it will endure during an aircraft's lifetime. The objective of this diploma thesis is the analyses of on the structural strength on cockpit furniture. ST3D, the engineering section of ST GROUP creates and tests cockpits in a virtual environment before they are built by ST COMPOSITES, the production sector. This thesis shows the engineering work on the centre pedestal with the focus on computer based testing by using the finite element methods. One critical component in the structural stability are joints and another aspect of this thesis is the precalculation of a joint's strength. This is undertaken roughly in an analytical way, more precisely with the finite element methods and compared by a series of tests. The components from the cockpits of two aircraft that have been actually developed serve as examples. A centre pedestal is analysed from the civil Airbus A350 and the joint analysis is undertaken for the A400M from Airbus Military.

The results of this thesis are that the maximum strength of joints can be predicted but with variances. These variances can be reduced by

- further equations for the analytical calculation
- modelling the geometry of the tenons and mortises for the numerical calculation
- determine the material values of the potting-honeycomb mixture

The centre pedestal was optimized successful so that the structure has an acceptable first natural frequency and structural weight. The static analyses show that a small zone of structure do not resist to all load cases. This can be adjusted by reinforcing this zone. An eventually further optimization in weight and/or natural frequency may be needed.

Contents

1	Introduction	7
1.1	ST GROUP	8
1.2	Aircraft	11
1.3	Composites	13
1.3.1	Composition	15
1.3.2	Mechanical properties	16
1.3.3	Processing	17
1.3.4	Sandwich	18
1.4	Analytical calculation basic knowledge	20
1.4.1	Basic values definition	20
1.4.2	Stiffness matrices definition	22
1.5	Software	27
2	Mortise and tenon joints	29
2.1	Materials	34
2.2	Finite element methods	38
2.3	Analytical calculation	42
2.3.1	Stiffness matrices	42
2.3.2	Analytical problems	46
2.3.3	Adhesive calculation	48
2.3.4	Sandwich panel calculation	48
2.4	Conclusion	53
3	The A350 centre pedestal with FEM	55
3.1	Modelization	55
3.1.1	Elements	60
3.1.2	Fixings	63
3.1.3	Properties	63
3.1.4	Export	65
3.2	Modal analysis	68
3.2.1	Theory	68
3.2.2	Optimization	72
3.3	Static analyses	79

3.3.1 Von Mises	79
3.3.2 Hill criterion	80
3.3.3 Honeycomb YZ-, ZX-Components	82
3.4 Conclusion	82
List of figures	86
List of tables	88
Bibliography	90
Appendix	92
NASTRAN element definitions	98
MAT1	98
MAT8	99
CONM2	101
CQUAD4	102
CTRIA3	104
PCOMP	106
PSHELL	108
RBE2	110
RBE3	111
SPC	113

1 Introduction

In the year 2009, Europe is developing two big aircrafts by the European Aeronautic Defence and Space (EADS) Companies Airbus and Airbus Military; the long range, wide body A350 Airliner and the A400M, a four-engine turboprop military transport and tanker. Their development is coordinated from Toulouse, France where the headquarters are based. The company ST GROUP is a subcontractor. It designs and builds cockpit furniture for AIRBUS. The furniture has to guaranty the resistance to all possible load cases during an aircraft life and at the same time, the aircraft components have to be as light as possible to reduce the kerosene consumption. The aeronautic and space industry applies more and more fibre-reinforced composites because of their good ratio of density to stiffness. Composites are not easy to calculate. This is in particular explained in the chapter of tenon and mortise joints.

Joints are critical subjects in the structural strength analyses of cockpit furniture (see chapter 2). This chapter shows the stiffness analyses, on the one hand by a physical test series, on the other hand by using the finite element methods (FEM) and finally by doing analytical calculation.

The following chapter does not deal with composite structure in detail but with its general analysis. It describes how a finite element model is built, analysed and optimized with the A350 centre pedestal as example. First, an analysis of the structure's natural frequency is done. Then, by manipulating the structure, the natural frequency is raised and the structure's stability is verified by a static analysis.

The chapter introduction gives background information about the applied materials and the way their stability is calculated. Furthermore, this chapter is about the finite element software NASTRAN/PATRAN that is used to analyse the cockpit structure, the company that develops and produces them and the aircraft for which these cockpits are made.

1.1 ST GROUP

ST GROUP is a global aerospace subcontractor and composite manufacturer. The group consists of ST-AERO, ST3D, and ST COMPOSITES. The company is based at Toulouse-Labège.



Figure 1.1: ST GROUP logo

"Toulouse is the home base of the European aerospace industry, with the headquarters of AIRBUS, Galileo positioning system, the SPOT satellite system, and CNES's Toulouse Space Centre (CST), the largest space center in Europe. Thales Alenia Space, Europe's largest satellite manufacturer, and EADS Astrium Satellites, EADS's satellite system subsidiary, also have a significant presence in Toulouse." [Wik01]



Figure 1.2: ST GROUP premises

ST GROUP is a first level supplier for AIRBUS. The development and construction of the A400M and A350 cockpit furniture and the centre pedestal of the A380 have been the main activities of the group. Furthermore as a composite manufacturer it designs any kind of composite structures like parts for satellites, cars and many more.

Today, the capital of ST GROUP increased to 650000 €. The turnover in 2008 was about 3.1 M€. ST3D acts now as supply company for ST-AERO. The company ST-AERO, also founded by Stephane Trento, was created to manage projects and contracts with clients. With the foundation of ST COMPOSITES, the production and assemblage is regrouped under another ST-AERO supply company.

ST3D - Design office and technical service

In 1998, Stéphane Trento, the current chairman and managing director, founded the society ST3D. As an engineering firm, ST3D develops parts for industrial clients. With its creation, ST3D had a statute of limited liability company which fixed assets was 8000 €. In January 2003, ST3D acquired the legal status of "Société par Actions Simplifiée" (S.A.S.).

The activity of ST GROUP is concentrated on aeronautics, the spatial, car industry, mechanical tools and other industrial products. ST3D is a design department and technical support firm. The main customers are AIRBUS, LATECOERE GROUP, LIEBHERR AEROSPACE, Alcatel Alenia Space, EADS Astrium, ALTRAN, AKKA, etc.

ST COMPOSITES - Composite parts manufacturer

With various technologies like monolithic carbon, RTM, heat-hardening and destructive/non-destructive test methods, the company is able to produce sub-assemblies as well as full work packages (WP). ST COMPOSITES is equipped with:

- 150 m^2 production and assemblage surface
- a test laboratory with a 100kN Instron compression machine
- two cool chambers with temperature surveillance
- 18 m^3 oven
- 23 m^3 autoclave
- 24 m^2 painting cabin

ST GROUP has about 50 employees (there will be 100 in 2010):

- 67% technicians
- 20% technicals experts
- 8% administration
- 5% engineers

[Gro09]

1.2 Aircraft

The development of aircraft components are subdivided in several phases. They are called MAT A, MAT B, MAT C and JUSTIF. MAT is the abbreviation for maturity and JUSTIF stands for justification. During phase MAT A the design department creates the furniture which then, is analysed by the stress department. During MAT B the design department uses the results of the stress analysis to adapt the structure. During MAT C the same process is used in a more detailed way. Phase JUSTIF is the last one where everything is prepared for the manufacture. The furniture of the A400M cockpit is already in phase JUSTIF while the changes on the A350 centre pedestal (see chapter 3) are made during phase MAT B.

The first five manufactured A400M aircrafts are prototypes, called MSN001 to MSN005. MSN stands for manufacturer serial number. Figure 1.3 shows the MSN001 under construction in the EADS CASA (Construcciones Aeronáuticas S.A.) factory of San Paolo, Madrid. The following sections give some background information about the aircrafts where the cockpits are employed.

An overview of the A350 and the A400M aircraft is given in the appendix from page 92 to 96.



Figure 1.3: The A400M MSN001 under construction [Mil09]

1.3 Composites

"Composite materials (or composites for short) are engineered materials made from two or more constituent materials with significantly different physical or chemical properties which remain separate and distinct on a macroscopic level within the finished structure." [Wik04]

Fibre composites have an optimal ratio between minimal weight and maximal stiffness and strength. They are used everywhere where it is important to economize weight, for example to reduce the fuel consumption. This is especially important for transportation systems like rail vehicles, ships, cars, motorbikes and of course for aerospace industry. The formula $E = 1/2 \cdot m \cdot v^2$ shows that the energy requirement decreases by reducing the mass. Composite material is not only used to economize fuel and electricity but also to increase velocity with muscular strength. Bicycles and miscellaneous sports equipments are made from composite material, like bobsleighs, hockey sticks and tennis rackets. Composites become more and more important. They are applied increasingly. For example 54% of the Airbus A350 will be of composite structure. The reinforcing of material by fibres is not a new technical solution but a solution of nature that came by evolution. Many examples can be found in nature, like wood, hemp or bamboo. Especially bamboo is known for its stability (see figure 1.4). With a microscope the fibre orientation of the cells can be seen in figure 1.5.

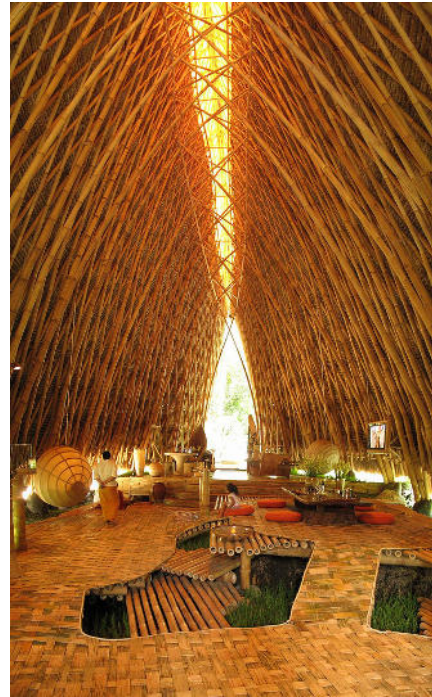


Figure 1.4: Bamboo structure [Fli08]

The advantages of fibre-reinforced materials are:

- high strength and high stiffness of material with a low density at the same time. That makes fibre-reinforced material an ideal material for lightweight construction.
- free shape design.
- excellent resistance against corrosion.
- the electrical conductance is adjustable.
- good heat insulating properties.
- high specific energy absorption capacity. Important for crash or impacts.

[Sch07]

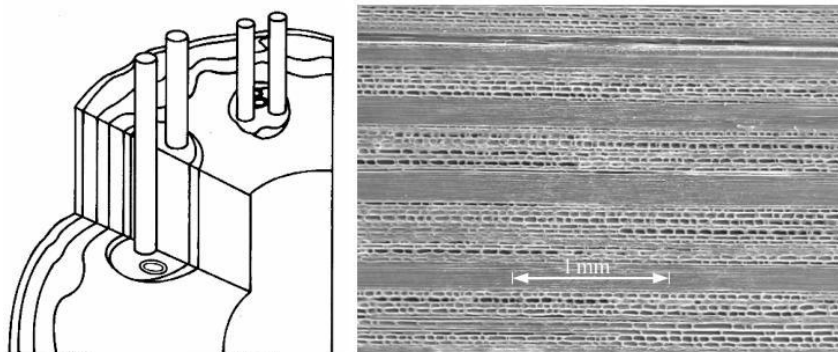


Figure 1.5: Left: Caulis of a plant. Right: Bamboo under microscope. The fibres are orientated like in fibre-reinforced composite. [Sch07]

1.3.1 Composition

The most primitive composite materials are straw and mud combined to form bricks for building construction. The most advanced examples are applied on spacecraft. The most visible are steel and aggregate reinforced cement or asphalt concrete. Even shower stalls and bath tubs are made of fibreglass. Composites are made up of two categories of constituent materials: matrix and reinforcement. The matrix material surrounds and supports the reinforcement materials by maintaining their relative positions. The special mechanical and physical properties of the reinforcements enhance the matrix properties. A synergism enables material properties that would be unavailable from the individual constituent materials. The wide variety of matrix and strengthening materials allows the designer of the product or structure to choose an optimum combination. Cockpit furniture for example, are made of preprags¹.

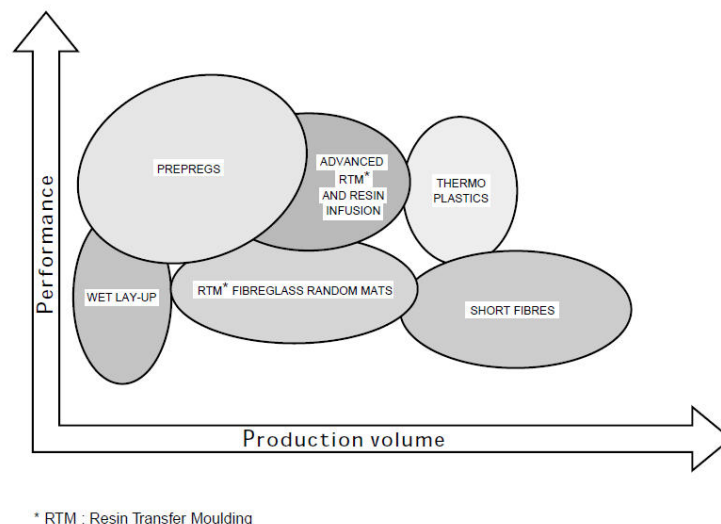


Figure 1.6: Different types of composites. [Hex09]

The matrix of most commercially produced composites are made of polymer material, often called resin solution. The most common are polyester, vinyl ester, epoxy, phenolic, polyimide, polyamide, polypropylene, PEEK, and others.

¹Preprags are a combination of a matrix and fibre reinforcement. They are ready to use in the component manufacturing process.

1.3.2 Mechanical properties

The strength of composites depends on the ratio of resin to fibre. In case of fibre glass reinforced preprags the ideal ratio is about 60% fibres and 40% resin. Compared to other materials like steel or aluminium, fibre reinforced composites have nearly no plastification zone. Thus, a rupture appears without visible announcement. It is also difficult to detect broken areas especially if they are tiny. Under tension the fibres rupture and under compression they buckle. If once an area is broken, even if it is a small area, the material does not support the same maximum stress any more. Also the crack can grow easily.

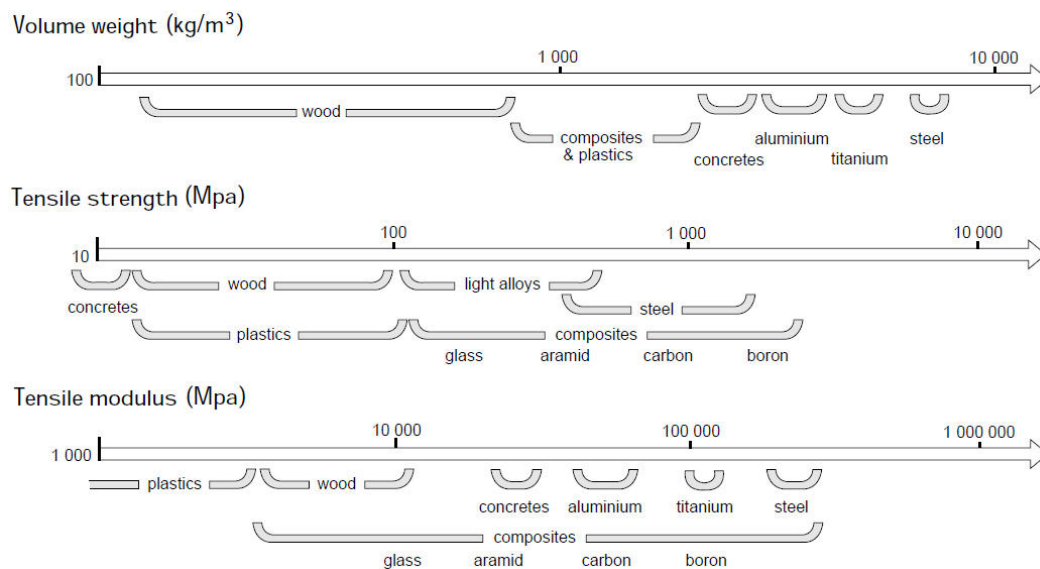


Figure 1.7: Composites provide the advantages of lower weight, greater strength and higher stiffness. [Hex09]

1.3.3 Processing

In general, the composite components are combined, compacted and processed to undergo a hardening event. After the hardening event, the part shape is essentially set. In general, for a thermoset² polymeric matrix material, the hardening event is a curing under high temperature. For a thermoplastic³ polymeric matrix material, the hardening event is a solidification. Cockpit furniture are second structure parts unlike primary structure, they do not have to support extreme stresses. A common way to produce composite parts is by using preprags. Cockpits are made of preprags and processed by the vacuum bag method. Figure 1.8 shows the preprag processing methods. Preprags are stocked at -18°C and have to be defrosted before shaping them at room temperature. Figure 1.8 shows the most common processing procedures.

Vacuum bag moulding The defrosted preprags are shaped by applying them onto a rigid mould. Before the curing in the oven, the construction is set under vacuum by wrapping it in a vacuum bag. This compacts the composite.

Autoclave moulding The processing is similar to the vacuum bag method. The difference to the oven is that the autoclave makes pressure. This enables a higher fibre volume fraction and a lower void content for high structural efficiency.

Resin transfer moulding (RTM) The resin transfer moulding does not apply preprags. The reinforcement is placed in the cavity of a two-sided mould. Then, resin is injected up to the fullness of the cavity.

Other methods Vacuum bag moulding, autoclave moulding and resin transfer moulding are the most common composites processing methods in the aviation industry. Other methods are match moulding process, pressure bag process and tube rolling process. These processes include preprags. Other methods without preprags are press moulding, transfer moulding and many more. There are also forming capabilities including CNC filament winding,

²plastic that hardens under high temperature

³plastic that can be shaped under high temperature

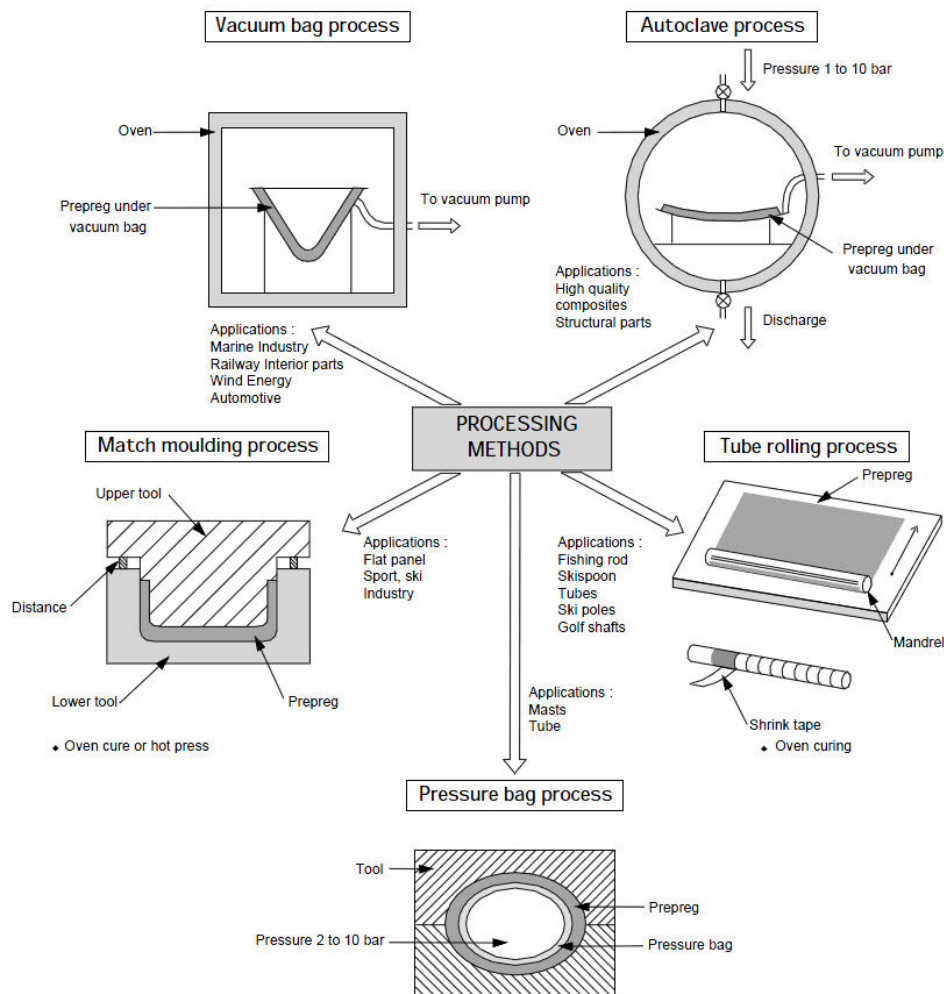


Figure 1.8: Different preprag processing methods [Hex09]

vacuum infusion, wet lay-up, compression moulding, and thermoplastic moulding. [Wik04]

1.3.4 Sandwich

Sandwich panels are becoming more and more popular in the construction industry due to their widespread structural applications in both commercial and residential building systems. In the widest sense a sandwich can be every multi-layered surface structure. But in the true sense a sandwich consists of

three layers: Two thin, stiff and strong sheets of dense material separated by and bonded rigidly to the centre core of lighter, weaker, less stiff and low-density material. The two thin sheets are usually called "faces" and the inner thick layer is called "core". Faces are commonly made of steel, aluminium or fibre reinforced composite material. The core material may be some sort of foam or a honeycomb structure (see figure 1.9). Figure 1.10 shows the efficiency of sandwich structure compared to composites without honeycomb. [Wie07] [KE06] [Gay97]

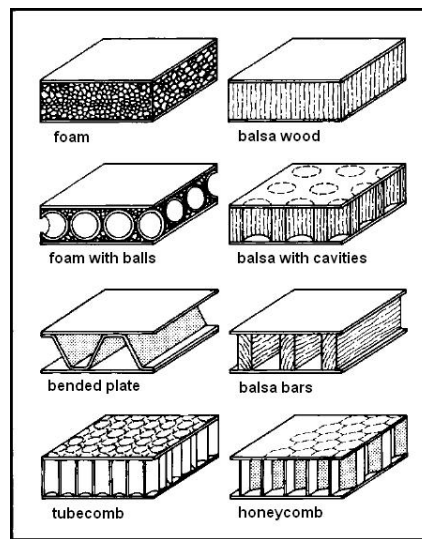


Figure 1.9: Different sandwich cores [Wie07]

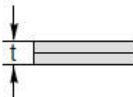
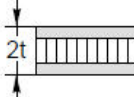

	Solid material	Core thickness t	Core thickness $3t$
			
Stiffness	1.0	7.0	37.0
Flexural strength	1.0	3.5	9.2
Weight	1.0	1.03	1.06

Figure 1.10: Sandwich compared to tissue composite [Hex09]

1.4 Analytical calculation basic knowledge

To be able to estimate the behaviour of composites it is necessary to have a stiffness matrix. To get this matrix, it is necessary to split up the composites in its pure components. So there are different levels to look at: The level of the multi-layered fibreglass, the level of one uni-directional fibreglass layer and the behaviour of pure fibre and pure resin. For sandwich structure there is also the sandwich level. In the following it will be shown how to obtain every needed value.

1.4.1 Basic values definition

Pure material values are given by the material manufacturer, see section 2.1 on page 34. In reality the fibreglass is a tissue with fibres orientated perpendicular to each other. But to calculate it the same way as the finite element solver NASTRAN, it is separated into two layers with half the thickness and a different orientation of 90°.

$E_{||}$ of a mixed layer of resin and uniaxial fibreglass Figure 1.11 shows the equation that is needed to obtain $E_{||}$. φ is the ratio between the volume of the fibres and the volume of the resin.

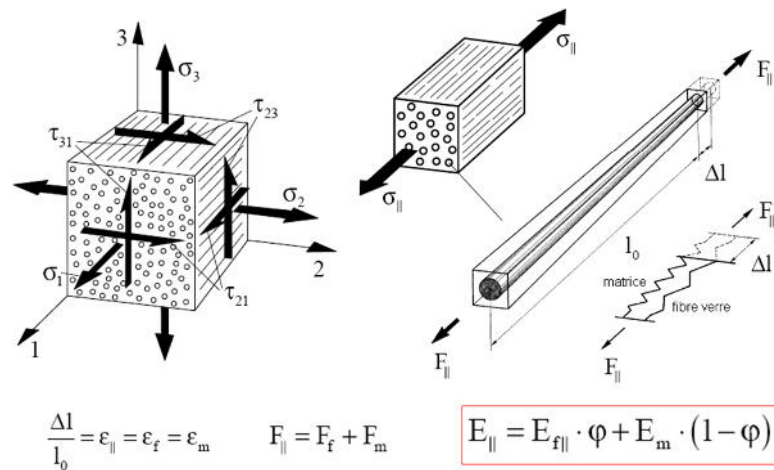


Figure 1.11: $E_{||}$ of a mixed layer of resin and uniaxial fibreglass

E_{\perp} of a mixed layer of resin and uniaxial fibreglass Figure 1.12 shows the formula that is needed to obtain E_{\perp} also named E_y . Because of the orthotropy the following equation is possible: $E_y = E_z$

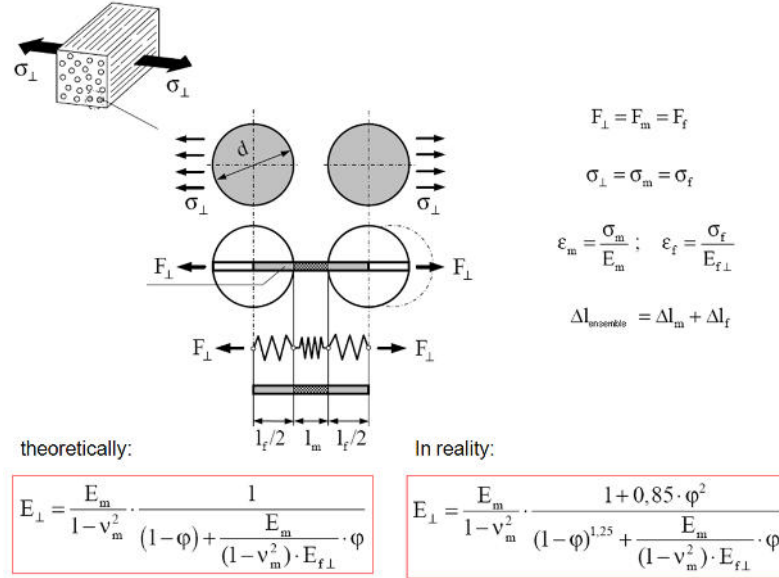


Figure 1.12: E_{\perp} of a mixed layer of resin and uniaxial fibreglass

$G_{\perp\parallel}$ of a mixed layer of resin and uniaxial fibreglass The formula for the $G_{\perp\parallel}$ is shown in figure 1.13.

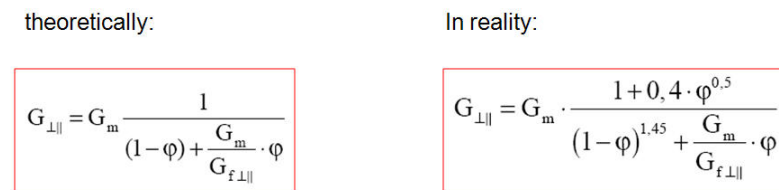
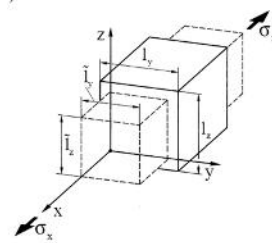


Figure 1.13: $G_{\perp\parallel}$ of a mixed layer of resin and uniaxial fibreglass

$\nu_{\perp\parallel}$ of a mixed layer of resin and uniaxial fibreglass The formula for the $\nu_{\perp\parallel}$ is shown on figure 1.14.



$$\tilde{A} = \tilde{l}_y^2 = l_y^2 \cdot (\epsilon_y^2 + 2 \cdot \epsilon_y + 1)$$

$$\epsilon_y^2 \ll \epsilon_y$$

$$\Delta A_m = \tilde{A}_m - A_m = A_m \cdot 2 \cdot \epsilon_y$$

$$\epsilon_x (= \epsilon_{||}) \quad v_m = -\epsilon_y / \epsilon_{||}$$

$$\left. \begin{aligned} \Delta A_m &= -2 \cdot v_m \cdot \epsilon_{||} \cdot A_m \\ \Delta A_f &= -2 \cdot v_{f \perp ||} \cdot \epsilon_{||} \cdot A_f \end{aligned} \right\} \Rightarrow \text{for one unidirectional (UD) ply} \quad \Delta A_{UD} = -2 \cdot v_{\perp ||} \cdot \epsilon_{||} \cdot A_{UD}$$

$$\Delta A_{UD} = \Delta A_f + \Delta A_m$$

$$-2 \cdot v_{\perp ||} \cdot \epsilon_{||} \cdot A_{UD} = -2 \cdot v_{f \perp ||} \cdot \epsilon_{||} \cdot A_f - 2 \cdot v_m \cdot \epsilon_{||} \cdot A_m$$

$$A_f / A_{UD} = \varphi \quad \text{et:} \quad A_m / A_{UD} = 1 - \varphi$$

$$v_{\perp ||} = \varphi \cdot v_{f \perp ||} + (1 - \varphi) \cdot v_m$$

$$\frac{v_{\perp ||}}{E_{\perp}} = \frac{v_{\perp ||}}{E_{||}}$$

Figure 1.14: $v_{\perp ||}$ of a mixed layer of resin and uniaxial fibreglass

1.4.2 Stiffness matrices definition

Honeycomb

The behaviour of a material is described by the elastical law containing the stiffness matrix [Q].

$$\begin{Bmatrix} \sigma_x \\ \sigma_y \\ \tau_{x,y} \end{Bmatrix}_{12} = \begin{bmatrix} Q_{11} & Q_{12} & Q_{16} \\ Q_{21} & Q_{22} & Q_{26} \\ Q_{16} & Q_{26} & Q_{66} \end{bmatrix}_{12} \cdot \begin{Bmatrix} \epsilon_x \\ \epsilon_y \\ \gamma_{x,y} \end{Bmatrix}_{12}$$

To describe the behaviour of the honeycomb as a homogeneous orthotropic material, basic values are implemented in the stiffness matrix as followed:

$$[Q] = \begin{bmatrix} \frac{E_{\parallel}}{1-\nu_{\perp\parallel}\cdot\nu_{\parallel\perp}} & \frac{\nu_{\parallel\perp}\cdot E_{\parallel}}{1-\nu_{\perp\parallel}\cdot\nu_{\parallel\perp}} & 0 \\ \frac{\nu_{\perp\parallel}\cdot E_{\perp}}{1-\nu_{\perp\parallel}\cdot\nu_{\parallel\perp}} & \frac{E_{\perp}}{1-\nu_{\perp\parallel}\cdot\nu_{\parallel\perp}} & 0 \\ 0 & 0 & G_{\perp\parallel} \end{bmatrix}$$

Fibreglass

After obtaining the basic values E_{\parallel} , E_{\perp} , G and $\nu_{\perp\parallel}$ of the fibreglass layer, the stiffness matrices for one layer are generated. The stiffness matrix of an orthotropic material is composed as follows:

$$[Q] = \begin{bmatrix} \frac{E_{\parallel}}{1-\nu_{\perp\parallel}\cdot\nu_{\parallel\perp}} & \frac{\nu_{\parallel\perp}\cdot E_{\parallel}}{1-\nu_{\perp\parallel}\cdot\nu_{\parallel\perp}} & 0 \\ \frac{\nu_{\perp\parallel}\cdot E_{\perp}}{1-\nu_{\perp\parallel}\cdot\nu_{\parallel\perp}} & \frac{E_{\perp}}{1-\nu_{\perp\parallel}\cdot\nu_{\parallel\perp}} & 0 \\ 0 & 0 & G_{\perp\parallel} \end{bmatrix}$$

We suppose that the first layer of the fibreglass ply is already orientated in the global coordinate system.

$$[\bar{Q}] = [Q]_{1,2}$$

The second ply is rotated by the angle of α . Therefore the stiffness matrix $[Q]_{1,2}$ and the strains $\sigma_{1,2}$ must be multiplied with the transformation matrix $[T]_{1,2 \rightarrow x,y}^{(\sigma)}$.

The 1,2-coordinate system of one UD-ply is:

$$\{\sigma\}_{1,2} = [Q]_{1,2} \cdot \{\varepsilon\}_{1,2}$$

Transformation of strains σ deformations τ of the 1,2-coordinates systems in the x,y-coordinate system.

$$\{\sigma\}_{x,y} = [T]_{1,2 \rightarrow x,y}^{(\sigma)} \cdot \{\sigma\}_{1,2}$$

$$[T]_{1,2 \rightarrow x,y}^{(\sigma)} = \begin{bmatrix} \cos^2 \alpha & \sin^2 \alpha & -\sin 2 \cdot \alpha \\ \sin^2 \alpha & \cos^2 \alpha & \sin 2 \cdot \alpha \\ 0,5 \cdot \sin 2 \cdot \alpha & -0,5 \cdot \sin 2 \cdot \alpha & \cos 2 \cdot \alpha \end{bmatrix}$$

Inclusion of the elastical law into the transformation correlation:

$$\{\sigma\}_{x,y} = [T]_{1,2 \rightarrow x,y}^{(\sigma)} \cdot [Q]_{1,2} \cdot \{\epsilon\}_{1,2}$$

By double transformation we obtain the transformed stiffness matrix $[\bar{Q}]$

$$[\bar{Q}] = [T]_{1,2 \rightarrow x,y}^{(\sigma)} \cdot [Q]_{1,2} \cdot [T]_{x,y \rightarrow 1,2}^{(\epsilon)}$$

$$[T]_{x,y \rightarrow 1,2}^{(\epsilon)} = \begin{bmatrix} \cos^2 \alpha & \sin^2 \alpha & 0,5 \cdot \sin 2 \cdot \alpha \\ \sin^2 \alpha & \cos^2 \alpha & -0,5 \cdot \sin 2 \cdot \alpha \\ -\sin 2 \cdot \alpha & \sin 2 \cdot \alpha & \cos 2 \cdot \alpha \end{bmatrix}$$

To handle the many different orientated layers of fibreglass together it is necessary to determine a global Young's modulus for each direction (E_x, E_y), a global shear modulus (G) and a global poisson's ratio (ν). With these global values it is possible to define the global matrix of the layer ensemble. But once the $[Q]$ matrices of each layer are defined, it is easier to skip the global-values-calculation and apply directly the mixture law to obtain one stiffness matrix for one global coordinate system. The equation is described as this:

$$[\hat{Q}]_{fiberglass} = \frac{\sum_{k=1}^n [\bar{Q}]_{xy,k} \cdot t_k}{t}$$

It is based on two conditions:

The global force is equal to the sum of forces on all layers as shown in picture 1.15

$$\{\hat{n}\} = \sum \{n\}_k$$

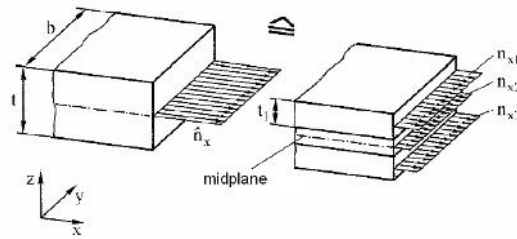


Figure 1.15: Equivalence of forces

with: $n = \frac{F_x}{b}$ where F_x represents the applied force and b represents the width of a layer

The rigidity of all layers is equal to the sum of rigidities of each layer.

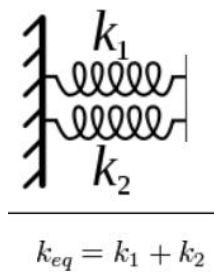


Figure 1.16: Equivalence of rigidity

$$k_{eq} = \sum k_i$$

Derivation of the correlation between the equivalence of forces, the equivalence of rigidity and the mixture law.

$$F = k \cdot \Delta x$$

$$\sigma = Q \cdot \varepsilon$$

$$\sigma = \frac{F}{S} = \underbrace{\frac{F}{b}}_n \cdot \frac{1}{t} = Q \cdot \frac{\Delta x}{x}$$

$$n = Q \cdot t \cdot \frac{\Delta x}{x}$$

$$n_k = Q_k \cdot t_k \cdot \frac{\Delta x}{x}$$

$$\{\hat{n}\} = \underbrace{[\hat{Q}] \cdot t \cdot \frac{\Delta x}{x}} = \sum n_k = \underbrace{\sum (Q_k \cdot t_k) \cdot \frac{\Delta x}{x}}$$

$$[\hat{Q}] = \frac{\sum (Q_k \cdot t_k)}{t}$$

Sandwich

The compound of a thin multi-layered upper fibreglass coat (uf), a thick honeycomb layer (hc) and thin multi-layered lower fibreglass coat (lf) can also be described in one stiffness matrix. To obtain it, it is the same procedure as for one multi-layered fibreglass panel: The application of the mixing law.

$$[\hat{Q}]_{sandwich} = \frac{[\hat{Q}]_{uf} \cdot t_{uf} + [\hat{Q}]_{hc} \cdot t_{hc} + [\hat{Q}]_{lf} \cdot t_{lf}}{t_{sum}}$$

Instead of $\{\sigma\} = [Q] \cdot \{\varepsilon\}$ another, more common way to describe a multi-layered material is:

$$\{n\} = \begin{bmatrix} [A] & [B] \\ [B] & [D] \end{bmatrix} \cdot \{\varepsilon\}$$

$$\begin{Bmatrix} n_x \\ n_y \\ n_{xy} \\ m_x \\ m_y \\ m_{xy} \end{Bmatrix} = \begin{bmatrix} A_{11} & A_{12} & A_{16} & B_{11} & B_{12} & B_{16} \\ A_{12} & A_{22} & A_{26} & B_{12} & B_{22} & B_{26} \\ A_{16} & A_{26} & A_{66} & B_{16} & B_{26} & B_{66} \\ B_{11} & B_{12} & B_{16} & D_{11} & D_{12} & D_{16} \\ B_{12} & B_{22} & B_{16} & D_{12} & D_{22} & D_{26} \\ B_{16} & B_{26} & B_{66} & D_{16} & D_{26} & D_{66} \end{bmatrix} \cdot \begin{Bmatrix} \epsilon_x \\ \epsilon_y \\ \gamma_{xy} \\ \kappa_x \\ \kappa_y \\ \kappa_{xy} \end{Bmatrix}$$

The advantages of NASTRAN are:

- often proved element- and result quality
- robust and efficient numerical methods for linear simulations
- quick calculations even on very big models
- adequate support through most model- and result processors

PATRAN is a preprocessor which is used to create finite element meshes. It is also a postprocessor which is able to show the results that were calculated by the solver NASTRAN. A created model under PATRAN is exported into an ASCII-file which includes all necessary information for the simulation. On the one hand the ASCII datasheet consists of a head which contains data about the way of calculation (static, dynamic, etc...) and what should be calculated (which kind of stress, displacement and element). On the other hand it includes the main part which consists of all used elements, its properties and locations. It also consists of the applied type of load and fixations. The layout of the PATRAN surface under UNIX is shown on figure 1.17. The figure shows also a typical error that appears if a material name is not entered properly.

2 Experimental, numerical and analytical analysis of mortise and tenon joints

This chapter shows how a structural strength analysis is done on joints by using the finite element methods with NASTRAN/PATRAN. It also describes the structural strength analysis with analytical calculation and the difficulties with it. Therefore the composites are viewed in detail. The focus here is on the L sample under tension and compression load.

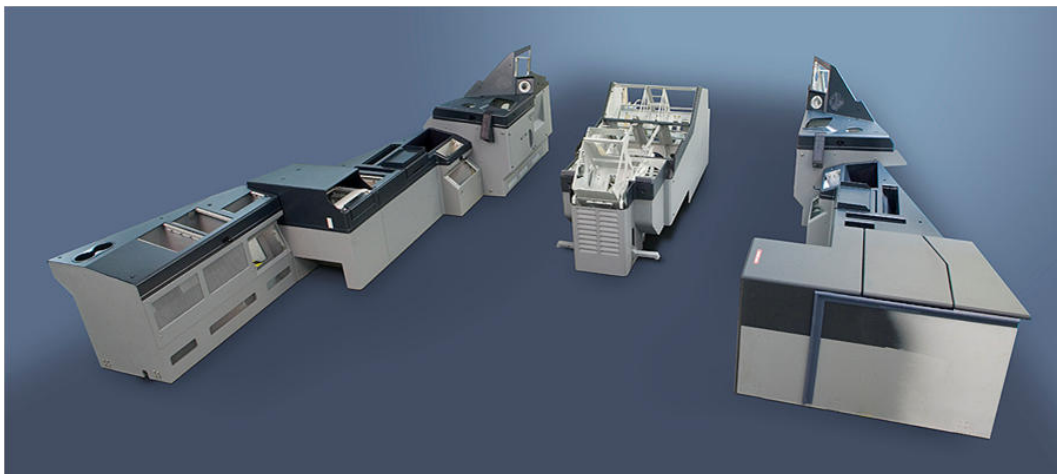


Figure 2.1: A400M cockpit furniture

The cockpit furniture is made of sandwich structure. Like in normal furniture the different wall units have to be connected. This is realised by equipping the wall units with mortises and tenons and stick them together. See figure 2.2. To keep the joint together, an adhesive is applied in between the two units.



Figure 2.2: The assembling of A400M cockpit furniture is done by sticking together the mortises and tenons in the production hall of ST Composites. The red circles signify two examples of the position of joints on the furniture. [ST3]

It is not possible to predict at which exact loads the joints will break. Nevertheless, to be able to design a cockpit, AIRBUS gives the maximum stress values (also called allowables) for those joints. These values are oversized to assure that the joints resist at least 100% of the values. To demonstrate that the manufactured joints of ST COMPOSITES correspond with the AIRBUS allowables, a test series has been started. Different panels can either be joined in T shape or in L shape. In addition, four layers of fibre glass tissue in L shape can be fixed with adhesive as reinforcement along the joints. An overview of different types of joints is given in figure 2.4 below. These samples are tested in different ways, under tension, compression and shear stress. See figure 2.5. The dimensions of the samples are shown in figure 2.3.

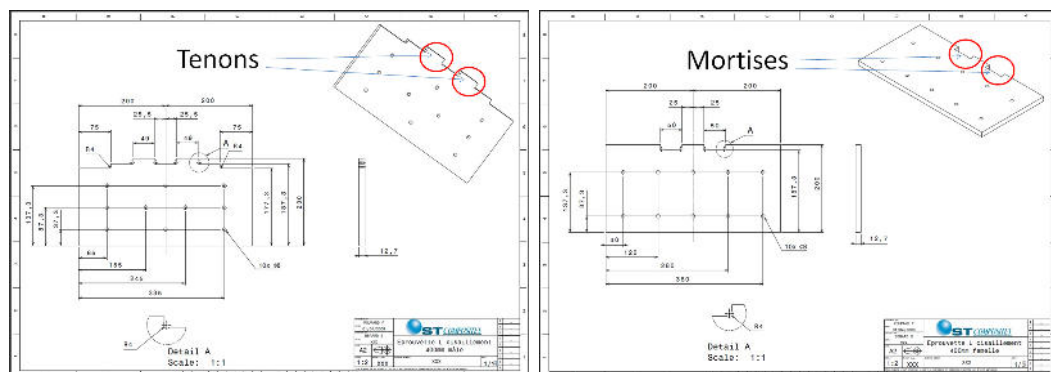


Figure 2.3: Sample dimensions

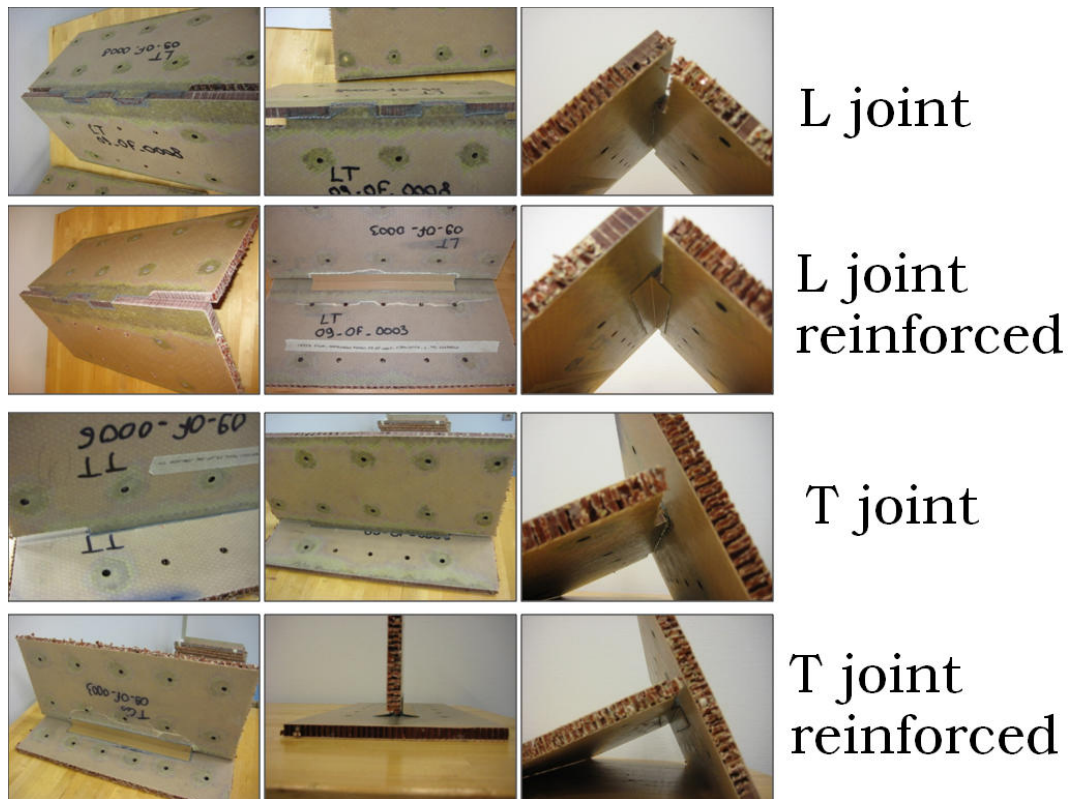


Figure 2.4: Tested joint types

Figure 2.6 shows the maximum supported stress (the allowables) of the L and T joints for tension, compression and shear load with and without reinforcement. Figure 2.7 shows at which force (in daN) the several samples cracked. Every load case has been tested on three samples. The average value is representative for every load case. The "Standard deviation" values show how precise the average values are. The field "AIF Admissible (N/mm)" lists the AIRBUS FRANCE allowables (see figure 2.6) which are multiplied with its length (250 mm) in field "Per length". The "Average(daN)" divided by the "Per length" gives the coefficient. The coefficient indicates how resistant the samples are compared to the AIRBUS allowables.

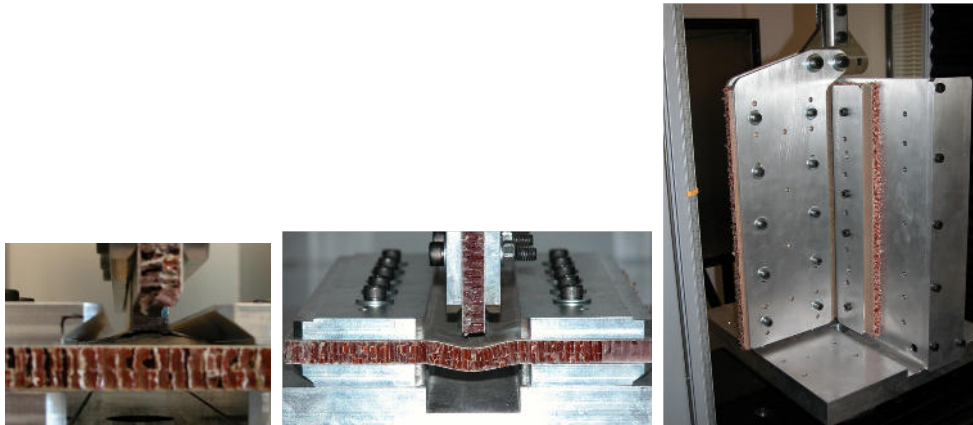


Figure 2.5: Different Load Cases; Left: tension; Centre: compression; Right: shearing

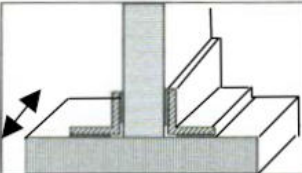
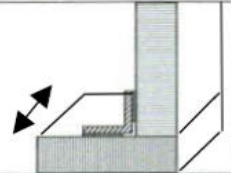
		 	
Configuration	Load	Configuration T	Configuration L
without reinforcement	Compression	11800 N/m	3500 N/m
	Traction	10800 N/m	4000 N/m
	Shear	34300 N/m	27100 N/m
with reinforcement	Compression	28000 N/m	10400N/m
	Traction	28000 N/m	6800 N/m
	Shear	34300 N/m	27100 N/m

Figure 2.6: Joint allowables provided by AIRBUS


	L Tenon Mortice samples				T Tenon Mortices samples			
	Test n°1		Test n°2		Test n°3		Test n°4	
	No reinforced		Reinforced		Noreinforced		Reinforced	
	Charge Max		Charge Max		Charge Max		Charge Max	
	Tensile		Tensile		Tensile		Tensile	
Sample 1	4	502	3	923	4	556	3	805
Sample 2	6	567	5	848	6	570	5	730
Sample 3	8	520	7	831	8	496	7	732
Average(daN)		529,7		867,3		540,7		755,7
Standard deviation		33,56		48,95		39,31		42,74
% Standard deviation		6,3		5,6		7,3		5,7
AIF Admissible (N/mm)		4,0		6,8		10,8		28,0
Por length		100,0		170,0		270,0		700,0
Coefficient		5,3		5,1		2,0		1,1
Compression				Compression				
Sample 1	4	387	3	1933	4	556	3	685
Sample 2	6	328	5	1150	6	570	5	701
Sample 3	8	375	7	1274	8	496	7	652
Average(daN)		363,3		1452,3		540,7		679,3
Standard deviation		31,18		420,86		39,31		24,99
% Standard deviation		8,6		29,0		7,3		3,7
AIF Admissible (N/mm)		3,5		10,4		11,8		28,0
Por length		87,5		260,0		295,0		700,0
Coefficient		4,2		5,6		1,8		1,0
Shearing				Shearing				
Sample 1	4	1901	3	1776	4	1842	3	2038
Sample 2	6	1844	5	1897	6	1764	5	1984
Sample 3	8	1671	7	1930	8	1609	7	1983
Average(daN)		1805,3		1867,7		1738,3		2001,7
Standard deviation		119,78		81,08		118,60		31,47
% Standard deviation		6,6		4,3		6,8		1,6
AIF Admissible (N/mm)		27,1		27,1		34,3		34,3
Por length		677,5		677,5		857,5		857,5
Coefficient		2,7		2,8		2,0		2,3

Figure 2.7: Test results

2.1 Materials

Sandwich The Sandwich structure is composed of fibreglass tissues and honeycomb made of aramid fibre paper. The outer layers, the skin, is made of two layers of fibre tissue and the core is made of honeycomb. See figure 2.8.

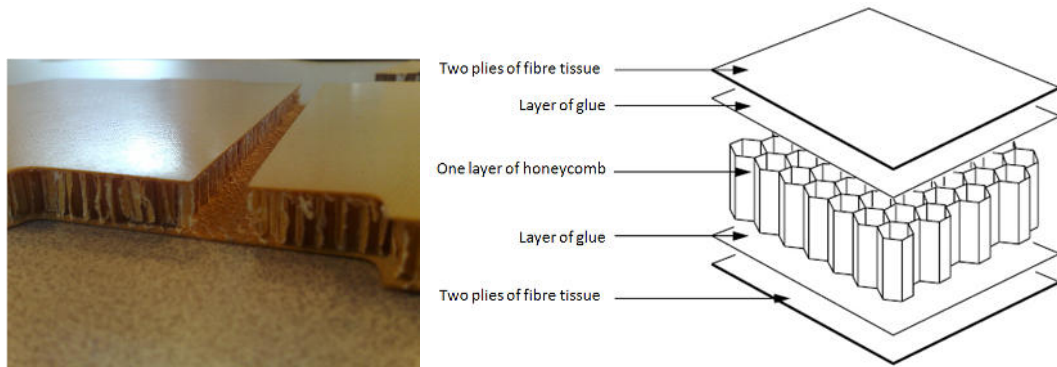


Figure 2.8: Sandwich material

Fibre reinforced tissue For the tests the Hexcel Fibre Glass Fabric 7781 8H Satin was used which is a regular fabric where every eighth string is superposed (see figure 2.9).

Table 2.1: Fibreglass tissue material data

Material type:	anisotropic
Density (prepreg):	$2,109\text{E-}06 \text{ kg/mm}^3 = 485 \text{ g/m}^2$
Mass ratio:	38% resin; 62% fibres
Thickness of one ply:	0,23 mm
Maximum torsion strength:	warp yarn = 500 MPa; fill yarn = 330 MPa
Maximum tension strength:	warp yarn = 500 MPa; fill yarn = 350 MPa
Maximum compression strength:	350 MPa
Flexion modulus:	warp yarn = 28 GPa; fill yarn = 21 GPa
Maximum shear strength:	40 MPa
Delamination force:	15 N/75 mm

Honeycomb The Hexcel HRH-10 3/16 3.0 is a regular honeycomb structure made of Nomex aramid-fibre paper recovered by a phenolic, fire resistant resin. 3/16 names the cell size in inch which is 4.8 mm. 3.0 names the density in pounds per cubic foot which is 48 kg/m^3 .

Table 2.2: Honeycomb material data

Structure:	orthotrop
Maximum compressive strength:	lonely = 2,0 MPa; stabilized = 2,3 MPa
Maximum shear strength:	L = 1,25 MPa; W = 0,6 MPa
Youngs Modulus:	140 MPa (stabilised)
Shear Modulus:	L = 41 MPa; W = 25 MPa

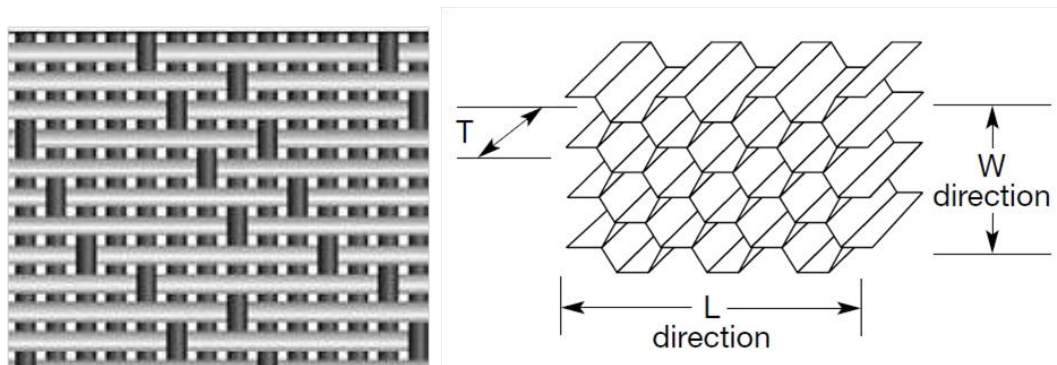


Figure 2.9: Left: The Eight Harness Satin pattern of the glass fibre tissue;
Right: The honeycomb structure

Adhesive The adhesive between the tenons and the mortises is shown in figure 2.10. It is a Henkel Hysol EA 9321. The distance between a tenon and a mortise is 0.5 mm.

Table 2.3: Adhesive material data

Material structure:	isotrop and thixotrop
Youngs Modulus:	$E = 2,9 \text{ GPa}$
Shear Modulus:	$G = 1,55 \text{ GPa}$
Poisson coefficient:	$\nu = 0,36$
Maximum compressive strength:	64 MPa
Maximum tension strength:	49 MPa
Maximum shear strength:	27,6 MPa



Figure 2.10: Mortises and tenons stuck together and fixed with Henkel Hysol adhesive

Potting One reason for the application of potting resin is to provide the structure from humidity. Potting is thixotropic paste that is formulated for edge filling of honeycomb sandwich construction. Another reason can be the reinforcement of the honeycomb structure, for example for the embedding of fixing supports (see figure 2.11) The technical data of potting is:

Table 2.4: Potting material data

Material structure:	isotrop
Density:	$6.73 \times 10^{-7} \text{ kg/mm}^3$
Youngs Modulus:	33965 MPa
Shear Modulus:	12769 MPa
Maximum compressive strength:	67.93 MPa

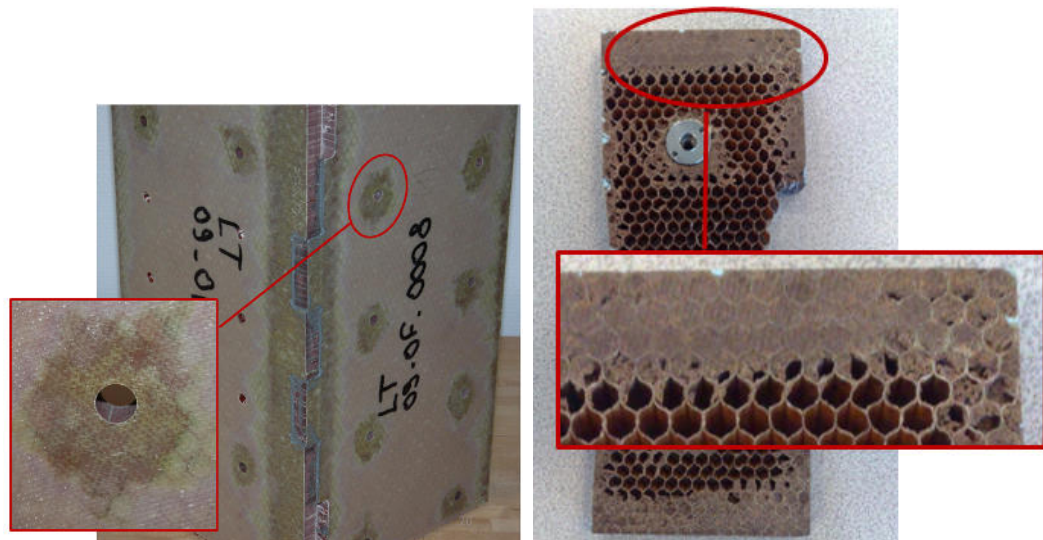


Figure 2.11: Potting inserted in honeycomb

2.2 Finite element methods

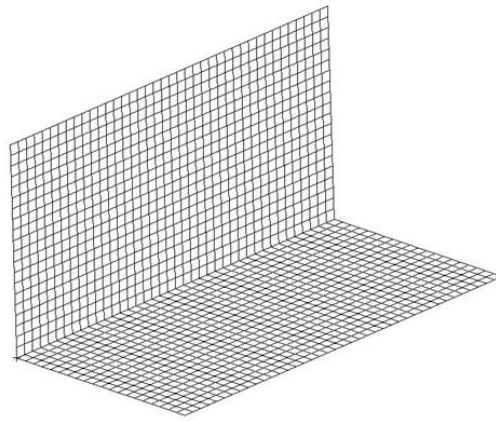


Figure 2.12: Finite element model of the L sample

The finite element methods are capable to calculate complex structures so they are used to calculate the joint structures.

Laminated Composite			
Stacking Sequence Convention			Offset
Total			-5.35
Stacking Sequence Definition			
	Material Name	Thickness	Orientation
1	1000002	1.150000E-001	0.000000E+000
2	1000002	1.150000E-001	9.000000E+001
3	1000002	1.150000E-001	0.000000E+000
4	1000002	1.150000E-001	9.000000E+001
5	1000001	1.178000E+001	0.000000E+000
6	1000002	1.150000E-001	9.000000E+001
7	1000002	1.150000E-001	0.000000E+000
8	1000002	1.150000E-001	9.000000E+001
9	1000002	1.150000E-001	0.000000E+000

Figure 2.13: Sandwich properties with PATRAN

A 2D model with CQUAD4 elements (for definition see appendix) is created. Near the joint the elements are smaller to get more precise results in this area. The nodes of the two grid planes do not touch each other. Instead, along the 250 mm joint the adhesive is represented by RBE2 elements (see figure 2.14) to observe the stresses that pass the joint. On the CQUAD elements the thicknesses and the sandwich material properties are applied. The constitution can be seen on figure 2.13. In NASTRAN/PATRAN every prepreg fibre glass fabric layer is splitted into two unidirectional 90° different orientated layers with half the thickness. NASTRAN applies itself the right theory depending

on the thickness of the elements material. Very thin plates are treated by the Von-Kármán theory, thin plates are calculated with the classical Kirchhoff-plate and thick plates, like sandwich, uses the Mindlin-Reissner-plate theory.

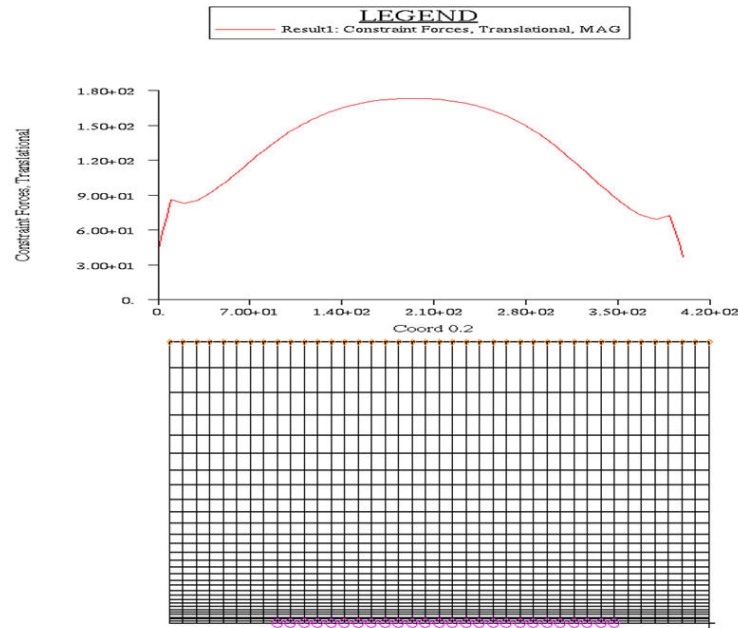


Figure 2.14: Finite element model with 2D elements. X-axis in mm; Y-axis in N

On the upper nodes of the model a displacement is applied. If different displacements are tested and the RF (definition in section "Reserve Factor" on page 40) is observed at the same time, it becomes clear that a displacement of 2 mm leads to an RF closest to the value 1. The top of figure 2.14 represents the constrain forces on the upper nodes of the grid which are necessary to obtain a displacement of 2 mm. All in all a force of 5216.8 N is required, without distinguishing the direction. That means that NASTRAN/PATRAN makes no difference whether the joint is loaded under tension or under compression.

Figure 2.16 shows the distribution of the Reserve Factor. The closer the RF value is to 1, the higher is the possibility that the structure cracks. If you change the scale (figure 2.16 left and right) you can see more easily where the L sample is going to crack first. In both cases, tension and compression, the model breaks in the same place. For the shear stresses inside the honeycomb layer, NASTRAN predicts no damage on this load case.

Reserve Factor (RF) It can roughly be said that RF is $\frac{\sigma_{max}}{\sigma_{real}}$. σ_{max} is the maximum supported stress of the material and σ_{real} is the actual stress that passes by the elements under the given load. If the RF value is below 1, the structure breaks, if it is above, it does not. In the industry this method is used to find oversized (and therefore too heavy) areas of parts by looking for too high RF values. With this method the structure can be optimized for the predicted loads and a maximum of weight can be saved. A more precise definition of the applied method is given in chapter 3.3.2 on page 80.

Results Figure 2.15 shows that the L sample breaks at exactly the area where NASTRAN predicts it. But it is not the weakest part. The potting-honeycomb mixture cracks before. This will be seen in the next chapter on page 52.

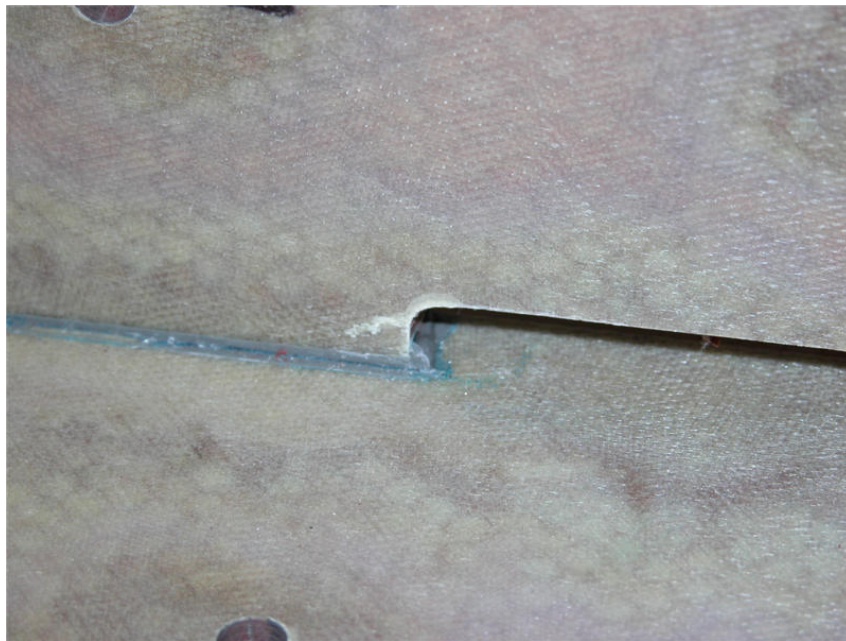


Figure 2.15: Damage on the L sample after compressive loading

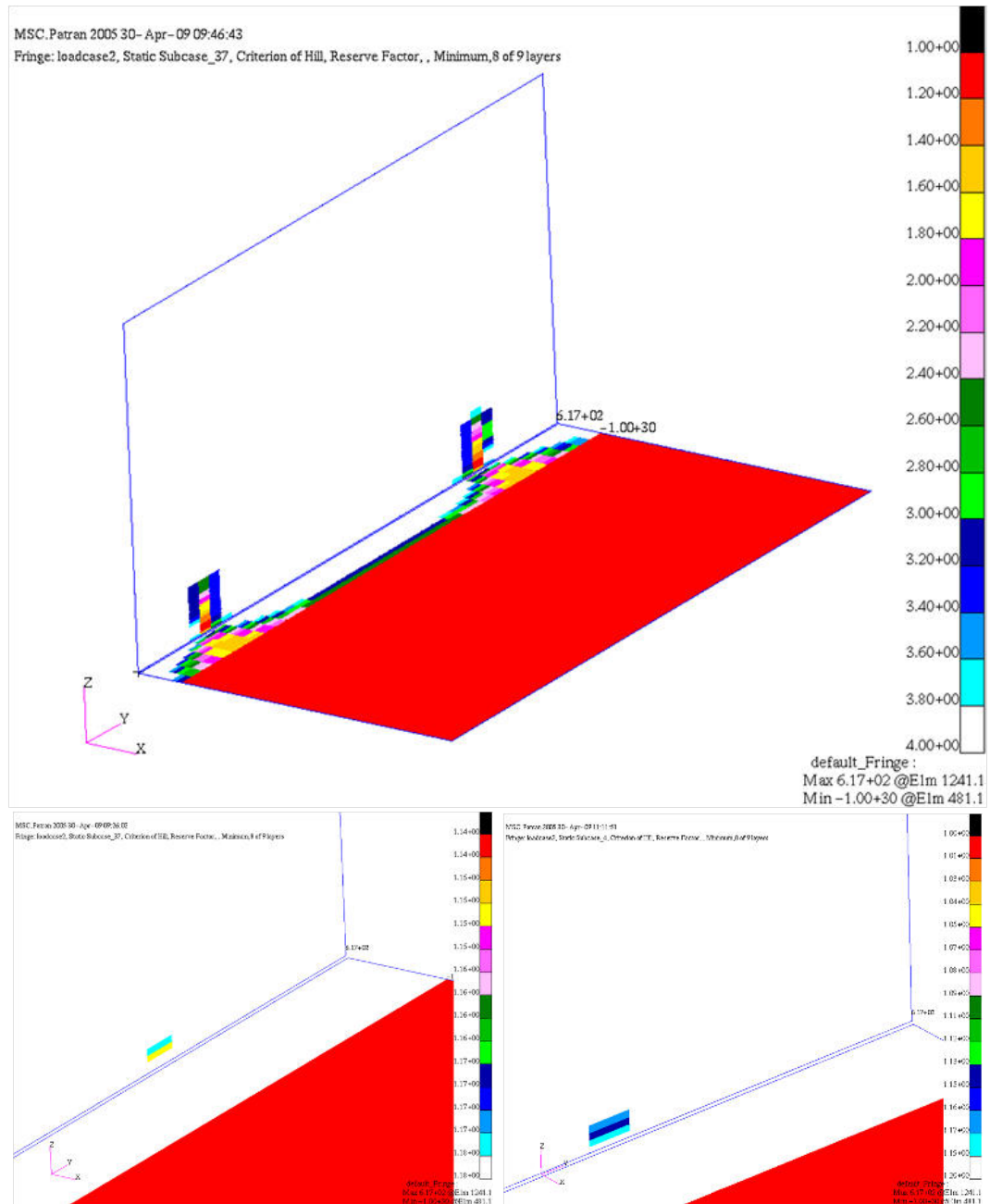


Figure 2.16: Top: RF distribution on L sample; Left: RF under tension; Right: RF under compression

2.3 Analytical calculation

2.3.1 Stiffness matrices

For the calculation of the stiffness matrix of each component, not the values from the manufacturer are applied but experienced data certificated by AIRBUS. After a certain time, for example 30 years, aircraft are no more allowed to fly because material gets weaker in time. This weakening effect is, amongst others, considered by these values. Airbus calculates a composite layer not as a fabric, but as two layers of uniaxial fibre preprags that are shifted at an angle of 90° (see figure 3.11). The uniaxial layers have half the thickness of the fabric layer.

Honeycomb

One ply of honeycomb:

$$E_{\parallel} = E_{\perp} = 0.01 \frac{N}{mm^2}$$

$$G_{1,2} = 0.1 \frac{N}{mm^2} ; G_{1,3} = 32 \frac{N}{mm^2} ; G_{2,3} = 24 \frac{N}{mm^2}$$

$$\nu_{\perp\parallel} = \nu_{\parallel\perp} = \nu_{\perp\perp} = 0.3$$

2D Matrix of one ply of honeycomb:

$$[Q]_{x,y} = \begin{bmatrix} 0.010989 & 0.0032967 & 0 \\ 0.0032967 & 0.010989 & 0 \\ 0 & 0 & 0.1 \end{bmatrix} \frac{N}{mm^2}$$

Fiberglass

One ply of fiberglass:

$$E_{\parallel} = 32500 \frac{N}{mm^2} ; E_{\perp} = 3000 \frac{N}{mm^2}$$

$$G_{1,2} = G_{1,3} = G_{2,3} = 3400 \frac{N}{mm^2}$$

$$\nu_{\perp\parallel} = 0.35 ; \nu_{\parallel\perp} = \nu_{\perp\perp} = 0.03230769$$

2D Matrix of one ply of fiberglass in its original coordinate system or rather with $\alpha = 0^\circ$:

$$[Q]_{1,2} = \begin{bmatrix} 32871.7 & 1062.01 & 0 \\ 1062.01 & 3034.31 & 0 \\ 0 & 0 & 3400 \end{bmatrix} \frac{N}{mm^2}$$

Sandwich

The sandwich structure is composed of one ply of multi-layered fiberglass on the top layer, one ply of honeycomb in the middle layer and one ply of multi-layered fiberglass on the bottom layer. To obtain the sandwich stiffness matrix, the matrix of each layer and multi-layer is needed.

In this case the upper and the lower fiberglass multi-layer is composed as same:

- One 0° UD-Layer
- One 90° UD-Layer
- One 0° UD-Layer
- One 90° UD-Layer

It is supposed that the first layer of the fiberglass ply is already orientated in the global Coordinate system. However the second ply is rotated by $\alpha = 90^\circ$. Therefore the stiffness matrix $[Q]$ and the strains σ must be multiplied with the transformation matrix $[T]_{1,2 \rightarrow x,y}^{(\sigma)}$.

$$[T]_{1,2 \rightarrow x,y}^{(\sigma)} = \begin{bmatrix} \cos^2 90^\circ & \sin^2 90^\circ & -\sin 2 \cdot 90^\circ \\ \sin^2 90^\circ & \cos^2 90^\circ & \sin 2 \cdot 90^\circ \\ 0,5 \cdot \sin 2 \cdot 90^\circ & -0,5 \cdot \sin 2 \cdot 90^\circ & \cos 2 \cdot 90^\circ \end{bmatrix} = \begin{bmatrix} 0 & 1 & 0 \\ 1 & 0 & 0 \\ 0 & 0 & -1 \end{bmatrix}$$

Until now the 1,2-coordinate system of one UD-ply is:

$$\{\sigma\}_{1,2} = [Q]_{1,2} \cdot \{\varepsilon\}_{1,2}$$

$$\begin{Bmatrix} \sigma_1 \\ \sigma_2 \\ \tau_{1,2} \end{Bmatrix}_{1,2} = \begin{bmatrix} 32871,7 & 1062,01 & 0 \\ 1062,01 & 3034,31 & 0 \\ 0 & 0 & 3400 \end{bmatrix}_{1,2} \cdot \begin{Bmatrix} \varepsilon_1 \\ \varepsilon_2 \\ \gamma_{1,2} \end{Bmatrix}_{1,2}$$

Transformation of stress σ deformations τ of the 1,2-coordinates systems in the x,y-coordinate system.

$$\{\sigma\}_{x,y} = [T]_{1,2 \rightarrow x,y}^{(\sigma)} \cdot \{\sigma\}_{1,2}$$

$$\begin{Bmatrix} \sigma_x \\ \sigma_y \\ \tau_{x,y} \end{Bmatrix}_{x,y} = \begin{bmatrix} 0 & 1 & 0 \\ 1 & 0 & 0 \\ 0 & 0 & -1 \end{bmatrix} \cdot \begin{Bmatrix} \sigma_1 \\ \sigma_2 \\ \tau_{1,2} \end{Bmatrix}_{1,2}$$

Inclusion of the elastical law into the transformation correlation:

$$\{\sigma\}_{x,y} = [T]_{1,2 \rightarrow x,y}^{(\sigma)} \cdot [Q]_{1,2} \cdot \{\varepsilon\}_{1,2}$$

$$\begin{Bmatrix} \sigma_x \\ \sigma_y \\ \tau_{x,y} \end{Bmatrix}_{x,y} = \begin{bmatrix} 0 & 1 & 0 \\ 1 & 0 & 0 \\ 0 & 0 & -1 \end{bmatrix} \cdot \begin{bmatrix} 32871,7 & 1062,01 & 0 \\ 1062,01 & 3034,31 & 0 \\ 0 & 0 & 3400 \end{bmatrix} \cdot \begin{Bmatrix} \varepsilon_1 \\ \varepsilon_2 \\ \gamma_{1,2} \end{Bmatrix}_{1,2}$$

$$\begin{Bmatrix} \sigma_x \\ \sigma_y \\ \tau_{x,y} \end{Bmatrix}_{x,y} = \begin{bmatrix} 1062,01 & 3034,31 & 0 \\ 32871,7 & 1062,01 & 0 \\ 0 & 0 & -3400 \end{bmatrix} \cdot \begin{Bmatrix} \varepsilon_1 \\ \varepsilon_2 \\ \gamma_{1,2} \end{Bmatrix}_{1,2}$$

By double transformation, the transformed stiffness matrix $[\bar{Q}]$ can be obtained.

$$[\bar{Q}] = [T]_{1,2 \rightarrow x,y}^{(\sigma)} \cdot [Q]_{1,2} \cdot [T]_{x,y \rightarrow 1,2}^{(\varepsilon)}$$

with:

$$[T]_{x,y \rightarrow 1,2}^{(\varepsilon)} = \begin{bmatrix} \cos^2 90^\circ & \sin^2 90^\circ & 0,5 \sin 2 \cdot 90^\circ \\ \sin^2 90^\circ & \cos^2 90^\circ & -0,5 \cdot \sin 2 \cdot 90^\circ \\ -\sin 2 \cdot 90^\circ & \sin 2 \cdot 90^\circ & \cos 2 \cdot 90^\circ \end{bmatrix} = \begin{bmatrix} 0 & 1 & 0 \\ 1 & 0 & 0 \\ 0 & 0 & -1 \end{bmatrix}$$

$$\begin{aligned}
[\bar{Q}] &= \begin{bmatrix} 0 & 1 & 0 \\ 1 & 0 & 0 \\ 0 & 0 & -1 \end{bmatrix} \cdot \begin{bmatrix} 32871,7 & 1062,01 & 0 \\ 1062,01 & 3034,31 & 0 \\ 0 & 0 & 3400 \end{bmatrix} \cdot \begin{bmatrix} 0 & 1 & 0 \\ 1 & 0 & 0 \\ 0 & 0 & -1 \end{bmatrix} \\
&= \begin{bmatrix} 3034,31 & 1062,01 & 0 \\ 1062,01 & 32871,7 & 0 \\ 0 & 0 & 3400 \end{bmatrix}
\end{aligned}$$

By applying the mixture law for two 0° and two 90° layers a stiffness matrix as followed is obtained:

$$[\bar{Q}]_{x,y4k-fiberglass} = \begin{bmatrix} 17953 & 1062,01 & 0 \\ 1062,01 & 17953 & 0 \\ 0 & 0 & 3400 \end{bmatrix}$$

By applying the mixture law for one ply of multi-layered fiberglass on the top layer, one ply of honeycomb in the middle layer and one ply of multi-layered fiberglass on the bottom layer, the sandwich stiffness matrix as followed can be obtained:

$$[\hat{Q}]_{x,y} = \begin{bmatrix} 1300 & 76.9 & 0 \\ 76.9 & 1300 & 0 \\ 0 & 0 & 246 \end{bmatrix} \frac{N}{mm^2}$$

2.3.2 Analytical problems

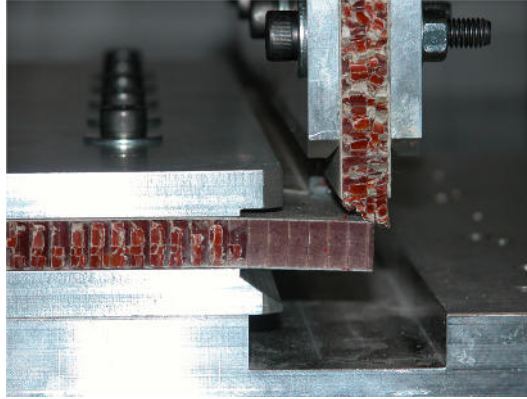


Figure 2.17: Deflection of the mortise sandwich panel of the L sample under compressive load

Irregular stress distribution For the L joint type the aim is to find an approximate formula that gives the maximum stress in the skin depending on the applied force $\sigma_{max}(F)$. Every fibre can at least support a tension σ_{max} which is also called $\sigma_{k,allowable}$. The $\sigma_{k,allowable}$ is given by the manufacturer. The σ in the material depends on the applied load or on the applied displacement ($F = k \cdot \Delta x$). For an isotropic cantilever e.g. it is defined by:

$$\sigma_x = \frac{M_y}{I_y} \cdot y_{max} = \frac{F_y \cdot x}{I_y} \cdot y_{max}$$

This is a linear equation like $y = a \cdot x + b$. Here the y would be σ_x , the a would be $\frac{F_y \cdot x}{I_y}$, the x would be y_{max} and the b is zero. The graphical plot of the distributed load in an isotropic cantilever is like in figure 2.18 in the centre. The distribution in a sandwich structure is not the same as it can be seen on figure 2.18. The left side shows a sandwich cantilever under flexion load. In the centre the homogenous displacement can be seen and on the left side the distributed stress is represented. So the maximum stress should be on the outer skins. A way to continue working on this project could be to find out the non linear equation of the stress distribution. So it would be possible to find F_y for the $\sigma_{allowable}$ of the fibreglass. Another problem is the effect of delamination that has to be considered. The L samples under compression delaminate on the lower skin of the sandwich panel (see figure 2.19).

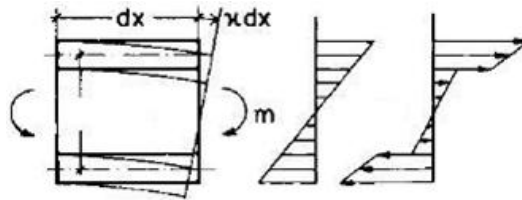


Figure 2.18: Left: Sandwich flexion under moment load; centre: The distributed displacement; right: The distributed stress

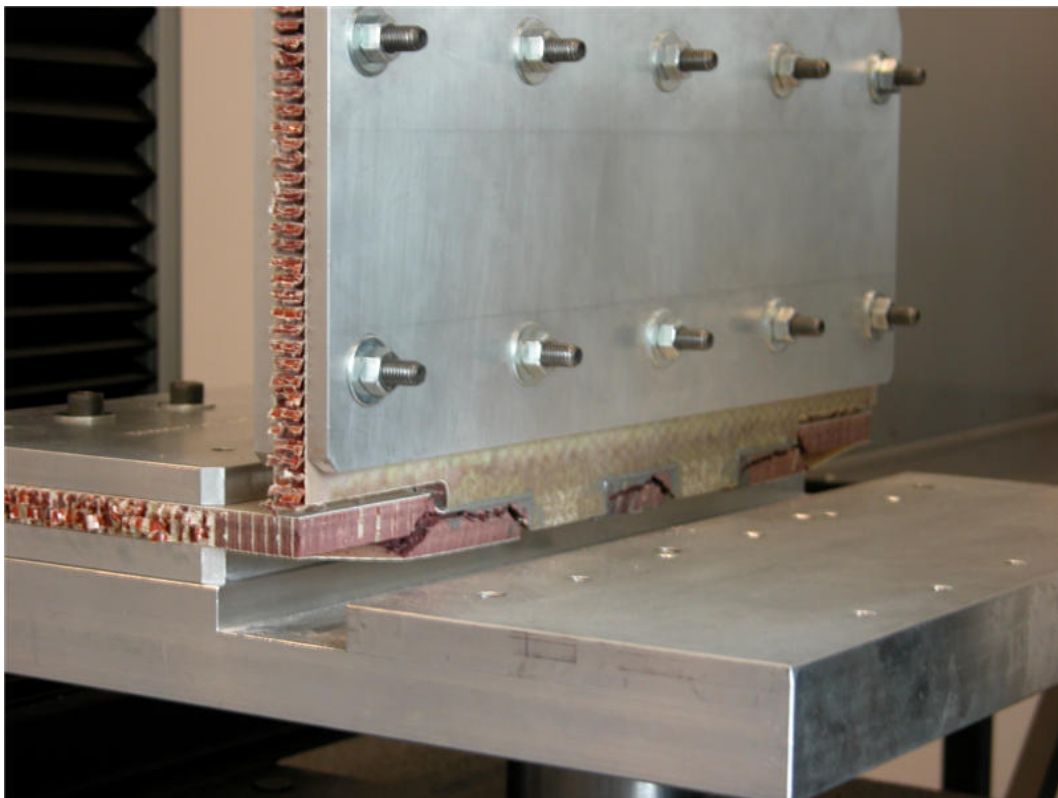


Figure 2.19: Delamination of the lower skin of L sample

2.3.3 Adhesive calculation

To find out if the adhesive resists to the load cases or if it is the weakest part of the joint, the maximum shear support is calculated. The L joint (under tension) is taken as example because it has the least glued surfaces. To obtain the maximum force that can be applied, the adhesive coated surfaces that are loaded under shear stress are added up and multiplied with the given maximum shear strength (27.6 MPa). The result shows that a 250 mm joint with 50mm tenons and mortises can support about 50 kN which means more than 200 N/mm. Compared with the AIRBUS maximum stress, which is 4 N/mm for tension, it can be loaded a lot more. Thus, during the stress tests the sandwich structure will probably be damaged before the adhesive fails.

2.3.4 Sandwich panel calculation

For sandwich structures, the bending part is only a 50th compared to the shear part. So the bending part is not considered but instead a tolerance of two per cent of the final result has to be accepted.

Furthermore in 1936 Raymond D. Mindlin found the so-called "Mindlin Problem" which proves that the y-z-surface of a bended, non-isotropic cantilever is not in a right angle with the deflection line. This means that the $\sigma_{x,sandwich}(y_{max})$ must be less than the $\sigma_{x,isotropic}(y_{max})$ of the Euler-Bernoulli beam equation. The reason for the lower tension in the upper and lower part of the bended beam is the lower angle.

The result of these two problems is that just the shear part will matter for further strength calculations. This also seems reasonable if you consider the small distance of 20mm between the fixed bearing and the vertical sandwich panel.

To simplify sandwich calculation AIRBUS documents offer some formulas:

The distribution of the shear stress is shown in figure 2.20

$$\tau_{max} = \frac{F}{\left(\frac{t_{upperfiberglass}}{2} + t_{honeycomb} + \frac{t_{lowerfiberglass}}{2}\right) \cdot b}$$

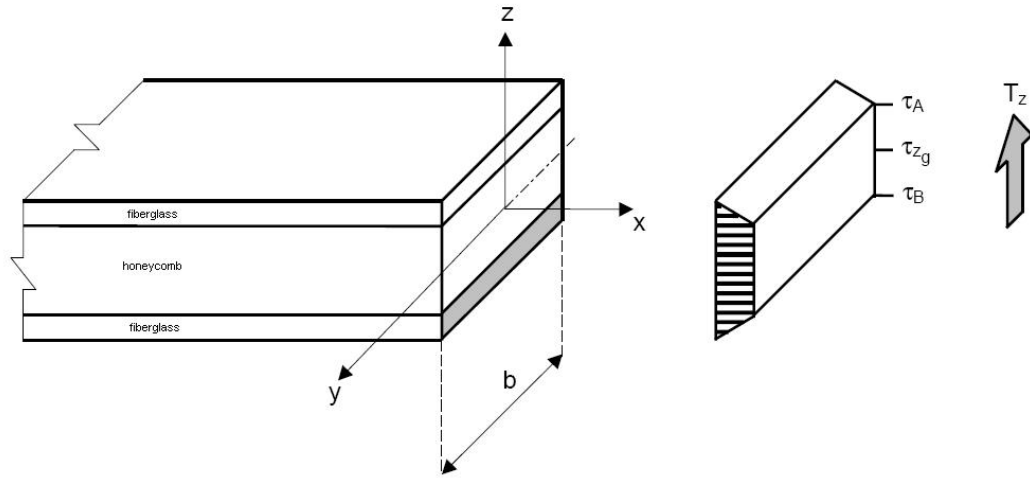


Figure 2.20: The distribution of the shear stress

To obtain the maximum force by a given $\tau_{max,honeycomb}$ the equation is changed to:

$$F_{max} = \tau_{max} \cdot \left(\frac{t_{upperfiberglass}}{2} + t_{honeycomb} + \frac{t_{lowerfiberglass}}{2} \right) \cdot b$$

This equation is valid for the loadcase of the L connection in tension and compression. For the loadcase on the T connection it is nearly the same equation but with a factor of 2. The applied force can be twice the force applied on the L connection because here it applies on two fixed bearings.

$$F_{max} = 2 \cdot \tau_{max} \cdot \left(\frac{t_{upperfiberglass}}{2} + t_{honeycomb} + \frac{t_{lowerfiberglass}}{2} \right) \cdot b$$

The distribution of the shear stress by an applied load in y-direction is shown in figure 2.21

The equation for this case:

$$\tau_{fiber} = \frac{3}{2} \frac{F_y}{b \cdot t_{fiber}} \frac{G_{fiber} \cdot t_{fiber}}{2 \cdot G_{fiber} \cdot t_{fiber} + G_{honeycomb} \cdot t_{honeycomb}}$$

To obtain the maximum force by a given $\tau_{max,fiber}$ the equation is changed to:

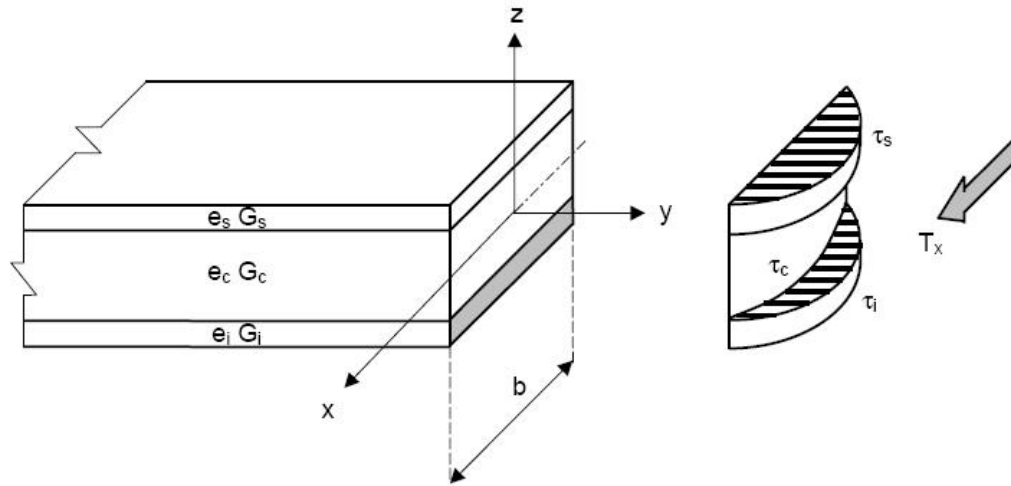


Figure 2.21: The distribution of the shear stress

$$F_{max,y} = \frac{\tau_{max,fiber} \cdot 2 \cdot b \cdot t_{fiber} \cdot (2 \cdot G_{fiber} \cdot t_{fiber} + G_{honeycomb} \cdot t_{honeycomb})}{3 \cdot G_{fiber} \cdot t_{fiber}}$$

Sample calculation of the L joint - tension/compression

The L bonding has a length of $b=250$ mm, a thickness of $t_{fiberglass}=0,46$ mm and $t_{honeycomb}=11,78$ mm. The $\tau_{allowable}$ for the honeycomb is $1,2N/mm^2$ in l-direction and $0,7N/mm^2$ in w-direction. The samples are made of w directed joints.

$$F_{w,max} = 0,7 \frac{N}{mm^2} \cdot \left(\frac{0,46mm}{2} + 11,78mm + \frac{0,46mm}{2} \right) \cdot 250mm = 2142N = 8,6 \frac{N}{mm}$$

Sample calculation of the T joint - tension/compression

The T bonding has also a length of $b=250$ mm, a thickness of $t_{fiberglass}=0,46$ mm and $t_{honeycomb}=11,78$ mm. The $\tau_{allowable}$ for the honeycomb is $1,2N/mm^2$ in l-direction and $0,7N/mm^2$ in w-direction. Again the w-direction is used.

$$F_{w,max} = 2 \cdot 0,7 \frac{N}{mm^2} \cdot \left(\frac{0,46mm}{2} + 11,78mm + \frac{0,46mm}{2} \right) \cdot 250mm = 4284 \frac{N}{mm^2} = 17,1 \frac{N}{mm}$$

Sample calculation of the L/T joint - shearing

The shear stress appears on the same dimensions for the L sample and for the T sample. So the results are the same for this calculation.

$$F_{max,y} = \frac{40 \frac{N}{mm^2} \cdot 2 \cdot 250mm \cdot 0,46mm \cdot (2 \cdot 3400 \frac{N}{mm^2} \cdot 0,46mm + 0,1 \frac{N}{mm^2} \cdot 11,78mm)}{3 \cdot 3400 \cdot 0,46mm} = 6136N = 24,5 \frac{N}{mm}$$

Results

Table 2.5 shows that calculated values are between the AIRBUS allowables and the test results for the tension and compression load case. This tells us that calculated values are sufficient for a predimension but not sufficient for the preview of exact structural behaviour. The results of the shear calculation have even a higher coefficient of security than the AIRBUS allowables. To construct with these values would lead to an oversized structure which would lead to a higher kerosine consumption than necessary.

Table 2.5: The calculated results compared with the AIRBUS allowables and the test results in $[N/mm]$

	L sample			T sample		
	Airbus allowable	Test result	analytical result	Airbus allowable	Test result	analytical result
tension						
Force $[N/mm]$	4.0	21.2	8.6	10.8	21.6	17.1
compression						
Force $[N/mm]$	3.5	14.5	8.6	11.8	21.6	17.1
shear						
Force $[N/mm]$	27.1	72.2	24.5	34.3	69.5	24.5

Figure 2.22 shows that the L sample breaks where the honeycomb and potting are mixed. Neither the adhesive nor the fibreglass of the sandwich structure fail.



Figure 2.22: The zigzag breaking line of a L sample under compression

2.4 Conclusion

Because of its composition of several materials in several order it is difficult to predict where and under which load a composite structure will break. Compared to isotropic structure, there are more criterias to be considered, like the delamination. So in fact, after obtaining the results of how the samples break, chapter 2.3.1 "Stiffness matrices" (page 42ff) and chapter 2.3.2 "Analytical problems" (page 46f) can be used for further calculations with these composites.

Neither the analytical nor the numerical calculation can preview the exact force at which the structure fails. The finite element methods predict that the structure cracks at 5216.8 N (20.9 N/mm) for compression almost as well as for tension (which is a deviation of about 1580 N for the compression load case and about 80 N for the tension load case). The reason for this is that the geometries of the tenons and mortises are not modeled and because of the difference between the maximum allowed tension stress and the maximum allowed compression stress which is only 5 MPa (355 MPa for tension and 350 MPa for compression) the results are almost the same in both cases. The different maximum loads between the compression load case and the tension load case of the test series can be explained by the effect of the delamination of the lower fibreglass skin of the mortise sandwich panel. Another source of error is that the calculations are done without potting. The used test samples in L shape that were loaded either under compression or tension break in the potting-honeycomb mixture first. The potting-honeycomb mixture is an orthotropic composite. It breaks on the three areas beside the mortises and inside the two tenons perpendicular to the l- and w-direction of the honeycomb.

To get more precise results, the maximum allowable shear strengths of the potting-honeycomb mixture have to be determined. This can be done by further test series for example with the INSTRON 100kN machine of ST COMPOSITES. To modelize the geometry, 3D elements could be applied. For example small HEX8 elements with a thickness of one or two fibreglass layers.

As already mentioned, composites are not easy to calculate. This is because of its complex composition. The safest way to know the limits of the stability of the composite structure is by making tests on real samples. To find an analytical way to predict breakage sufficiently close to the reality may be possible but means a lot of work. It should be proved if this is really necessary or if it

is not easier to make test series with samples.

3 The A350 centre pedestal with FEM

This chapter describes how nowadays aircraft structure is tested and optimized before being manufactured. To predict if the structure of the plane resists to all possible loads during an aircraft life, the industry uses finite element methods. The advantage over the analytical calculation is that arbitrary structure can be analysed with acceptable results. This chapter shows how a finite element model is created based on a CAD model, how it is analysed and how the optimization process works.



Figure 3.1: Left: A350 cockpit preview [Fli09]; Right: ST3D center pedestal CAD model

3.1 Modelization

The CAD model of the centre pedestal (shown in figure 3.1 right) is given by the design department of ST3D. They designed it with CATIA V5. CATIA is a CAD software developed by the French company Dassault System. Meanwhile it has become the most established software in France concerning aeronautical CAD modelling. The coarse design guidelines were given by Airbus. If

important changes have to be done on design, they have to be confirmed by Airbus. The centre pedestal consists of three parts, the outer structure (also called main structure) which reminds of a shell, the inner support structure labeled as canvas and the metallic frame which holds the control system devices. Except this frame, the pedestal is made of fibre reinforced composites. In general the centre pedestals of aircrafts were made of aluminium but for A350 a composite type might be deployed. Figure 3.2 shows which material has been applied at which area on the origin model.

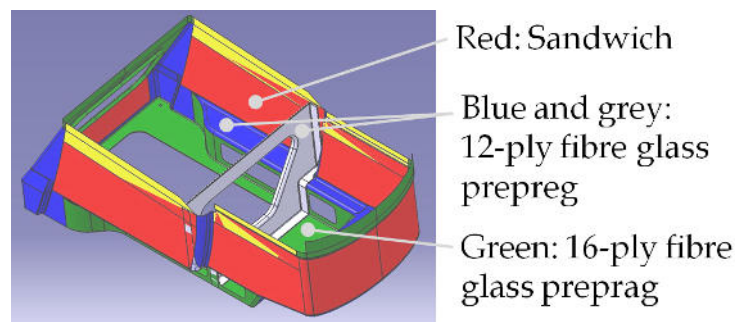


Figure 3.2: The original given thickness

To use this virtual 3D structure as a finite element model it has to be transformed. The finite element model will be a surface mesh with shell elements, where every element gets attributes like thickness and material properties. To create such a mesh the correct surface structure of the model is needed, so the CAD model has to be reduced from a volume structure to a surface structure. Every 3D structure has to be represented by a midplane surface when the thickness is applied symmetrically which is the case here. This becomes difficult if the structure gets more complex, like the metallic frame that can be seen on figure 3.3. In this case the structure has to be simplified by reduction before the midsurface will be created. This modification can be equalized by adding a non-structural mass (NSM). See paragraph "Non structural mass" on page 64.

Model simplification is done mainly to save time. Today, in times of globalization and thus worldwide competitions, to be efficient the industry tries hard to work not as good as possible but as good as needed. Thus to offer lower prices, every unnecessarily paid engineering working time has to be saved. To represent the shape in a very detailed way means to increase the number of elements and thus the time to calculate the model. It also means to investigate

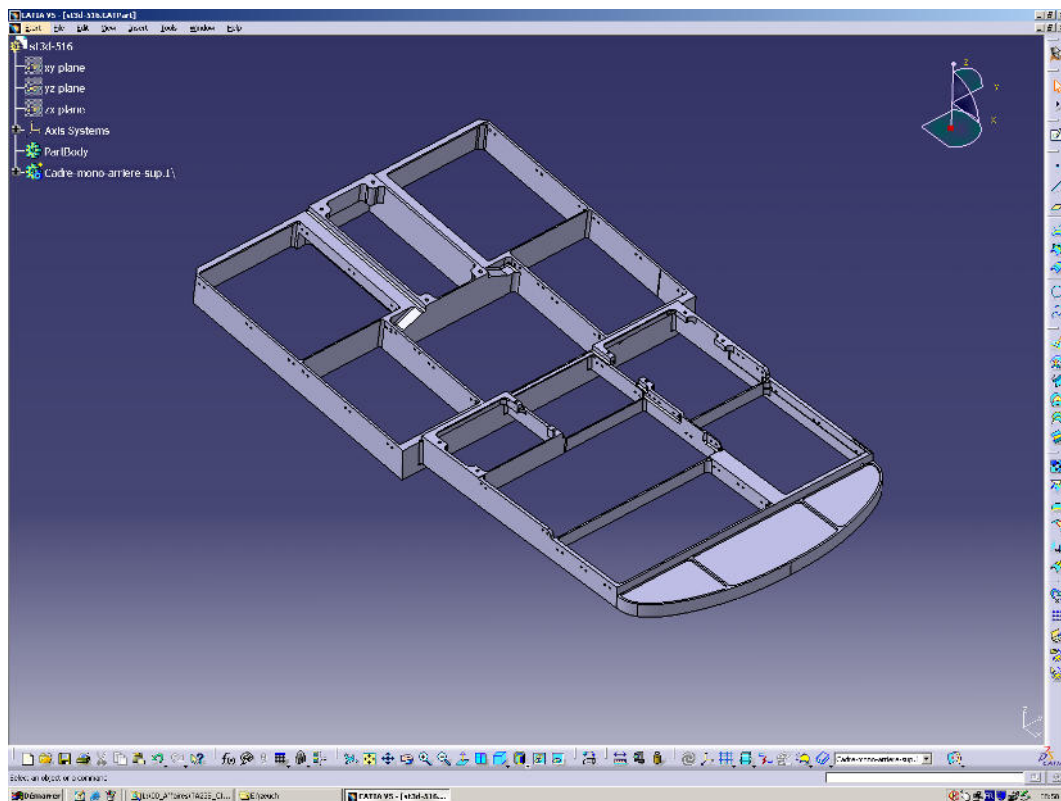


Figure 3.3: Metallic frame under CATIA V5

more time in midplane creation and in mesh creation. Model simplification is done in different varieties on the metallic frame. The rounded off edges between perpendicular surfaces have been neglected. They are replaced by 90° corners which permit to create a continuous mesh with related nodes between these two surfaces. This modification decreases the rigidity and increases the probability of crack formation. It can be seen as dispensable increase of safety factor. The variation can easily be ignored because their effect on the final results will be relatively unimportant. Furthermore small varieties of planes have been ignored; every surface is plane and has the same thickness (see figure 3.5) Holes are not considered. Holes are made to fix the electric equipment to the metallic frame. The representation of these fasteners is not necessary, the explanation is given in paragraph "0D mass elements" on page 62. In general the geometry is kept as simple as possible without too much deviation from the given structure. If the model should not be detailed enough it still can be improved later.

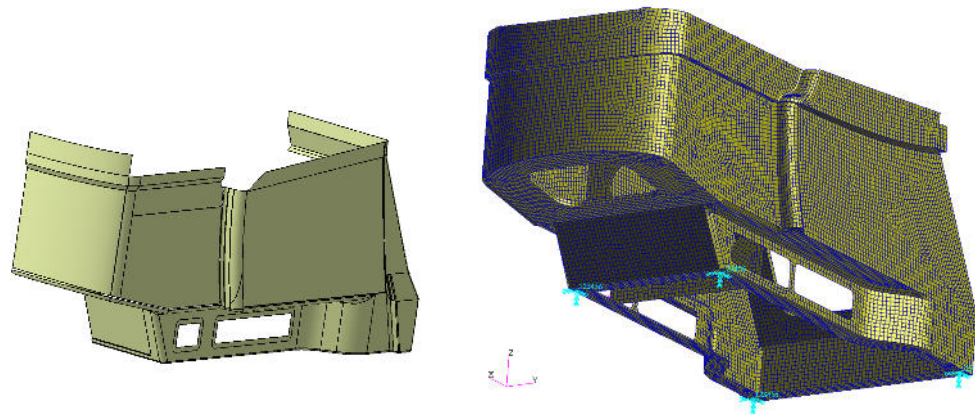


Figure 3.4: Left: CAD midplane surface model by using the symmetry; Right: Fixations

Midplane creation is made by moving either the inner or the outer face of a 3D surface towards the middle by employing an offset of half the thickness. The difficult part is the reconnection of separated surfaces which were connected properly as a 3D model but there could be mistakes with offset surfaces. If the midplanes overlap, the jutting out parts have to be cut, but if there is a gap in between, it has to be filled either by adding fill-surfaces or by connecting them directly with shell elements. There are different ways to reduce CAD models. In this case the midsurfaces are built with CATIA. An alternative would be to export the original CAD pedestal to edit it with the FEM software or even to rebuild it completely in accordance with the CAD dimensions. But the most efficient option is to edit the structure with CATIA which is programmed for design editing.

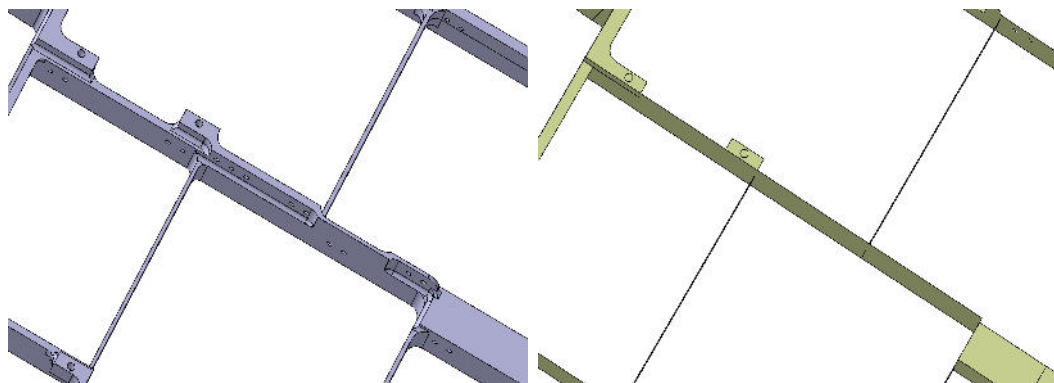


Figure 3.5: left: Volume structure; right: Midplane structure

Translation between CAD and FEM Software is possible by using the IGES interface. The Initial Graphics Exchange Interface (IGES) defines a neutral data format (*.igs) that allows the digital exchange in the form of points, lines, surfaces and solids. To import a 3D solid, the CAD model has to be created as a 3D solid. This is not the case here. Once the midplane model is created it is exported as *.igs file from CATIA. Under PATRAN you import the surfaces from this file as geometry. Geometry is needed to create a mesh. Once the mesh is created the geometry is not needed any more and can be deleted.

3.1.1 Elements

Mesh creation can be done once the surfaces are imported into PATRAN. The mesh consists of square shell elements. Their location is orientated on one global coordinate system placed on the nose of the plane. Every finite element aircraft component must have the same global coordinate system to assure that everything is on the right place when finally everything is put together. The square shell elements are generated automatically on the midplane surfaces with the "paver" option. The element dimension is set up to 8 mm x 8 mm. "Paver" means that the finite element software creates the mesh automatically on the chosen surface in order to keep the given element dimension as exactly as possible. Sometimes, especially if there are unnoticed small edges on a surface, caused by the CAD model, the paver option creates unnecessary small elements (see figure 3.6 left and centre). In this case those elements were deleted and replaced manual by larger elements to obtain a continuous and clear mesh.

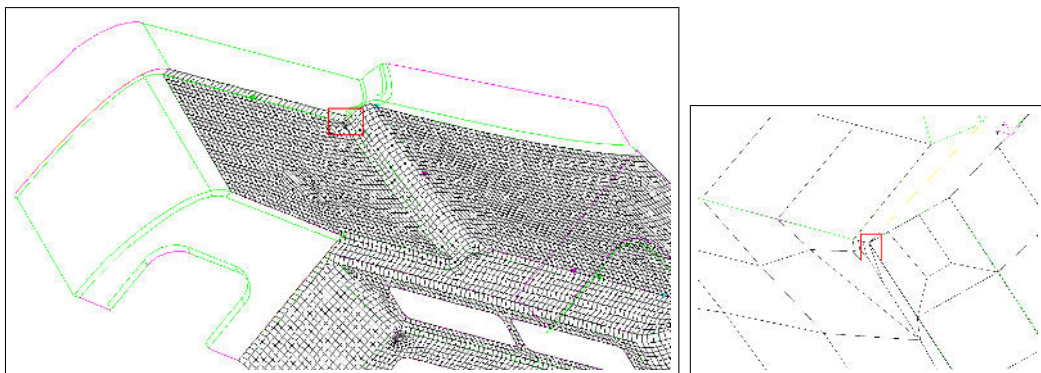


Figure 3.6: Errors in the "paver" option; Left: Centre pedestal during mesh creation; Right: Zoom on the red square of the left figure showing too small elements

Gaps. You have to distinguish between large gaps and thin gaps. If it is possible to connect different meshes by stretching the elements then these are thin gaps (see figure 3.6 right). But if elements have to be created between the two meshes you talk about large gaps. To handle the large gaps between surfaces there are two procedures. One procedure is to create surfaces between them, to associate the surfaces, to mesh them and to connect the meshes by the option "equivalence" where superposed nodes can be found and united

in a defined radius. Another procedure is to create the elements one by one using the available nodes of the two meshed midplanes. Whenever possible you create CQUAD4 elements (definition in appendix). Otherwise, if the number of nodes is not equal on both sides of the gap, you can also use CTRIA3 elements (definition in appendix) but the number of these elements should be kept as low as possible because the displacement answer of triangle elements is too rigid. If the gaps between meshed surfaces are thin, you can use the option "equivalence" in an expanded way. It is possible to determine the area where the "equivalence" should be applied (this would be the nodes of the meshed edges of the gap) and to widen the radius so that the meshes were "sewn" automatically. But be aware not to apply this method on gaps that are larger than the length of your elements otherwise the existing meshes can be damaged. One further solution is to use the option "move node" where elements can be connected manually one by one by stretching them. If there is no gap, the edges of two touching surfaces have to be joined by the option "associate". This assures that the nodes of both surfaces are superposed on the same edge. If this option is refused, the surfaces are probably separated by a non visible gap.

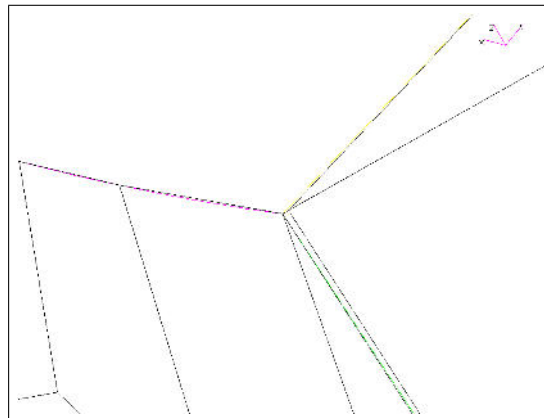


Figure 3.7: Zoom on the red square of figure 3.6 right showing a thin gap.

Once the mesh is created it has to be verified to be continuous without overseen gaps or overlapping elements. A helpful setting in PATRAN is "free edges". This permits to see just the mesh edges thus inconspicuous gaps or double elements can be discovered immediately. To correct irregularities the setting "equivalence", "move node", "delete element" or "create element" can be used. If the whole grid is proper, the elements have to be reviewed. Three kinds of checks are necessary; every element normal vector has to point in the same direction and every element has to respect the "taper ratio" and the

"skew angle" to make sure that no element is too skewed to provoke imprecise results.

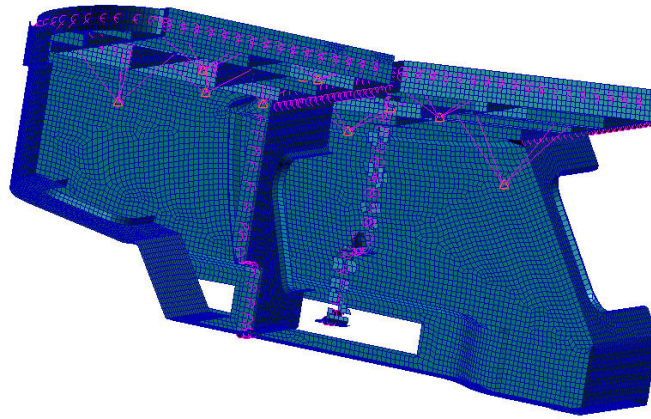


Figure 3.8: RBE elements on the finite element model

RBE2 are rigid elements that are used to connect different parts. Here these elements replace the glue between the metallic frame or the canvas and the main structure. The RBE2s are placed between one node (master) on the main structure and the nearest node (slave) on the frame or canvas structure. They transmit the displacements and rotations from the master node to the slave node (see figure 3.8).

RBE3 is an element like the RBE2. The difference is that not displacements but forces are transmitted. It is not a rigid element like RBE2. RBE3 elements are used to connect the masses of the electrical equipment with the metallic frame. They connect the punctual mass, which represents the electrical devices (see 0D element on page 62) with the metallic frame.

0D mass elements are used to represent the mass and the inertia of the equipments. Beside the CAD files the dimensions and weight of the electronic devices are given by Airbus. The inertias of each device are calculated by the formulas shown in figure 3.10. In PATRAN the 0D elements are nodes tagged with a triangle symbol (see figure 3.8).

3.1.2 Fixings

Fixings are modelled by constraining the corresponding nodes in translation and rotation. The pedestal is fixed on four points on the cockpit ground into rails. To keep the exact positions of the fixings their holes were not deleted by the process of model simplification (see "Model simplification" on page 56) and a node is created in its centre. This node is connected with the grid by manually added square elements.

3.1.3 Properties

Every element is allocated by a property which defines the used material and the shell thickness. The materials applied on the centre pedestal structure are defined as linear elastic and by values like Young's Modulus, Poissons Ratio and density. Aluminium is an isotrop material so the values are equal for each direction. Isotropic materials are defined as MAT1 in the NASTRAN datasheet. Orthotropic materials like uniaxial fibre glass prepreps and honeycomb are MAT8. If an element represents a composite structure like sandwich or multi-layered fibre glass it will be a PCOMP and will contain the names and orientations of the materials it is made of. Non-composite structures are called PSHELL. The definitions of the elements are given in the appendix.

Modifications should be kept as rarely as possible. In big assembly with several parts like aircrafts, changes happen frequently and are part of engineers working life. Even by using groups (see next paragraph), depending on the change, it can be very time-consuming. So it is important to get all information about the last state from all departments working on this project before beginning with modelling. During the project of the centre pedestal several changes in structure have been made. For example the following items have been changed:

- the dimensions of the lower windows
- the design of the metallic frame

- the design of the low, front part on both sides
- the upper all round border reduced in height

(compare figure 3.4 left with figure 3.4 right).

Groups under PATRAN are made to separate the whole mesh into different groups of meshes. This helps to keep the overall view and makes it easy to work on several areas with several elements without being confused or limited by temporary unneeded elements. The centre pedestal is separated into the following groups:

- metallic frame
- metallic frame connection (RBE2s)
- canvas left side
- canvas mirror
- canvas connection (RBE2s)
- main structure left side
- main structure mirror
- electrical devices (CONM2s and RBE3s)

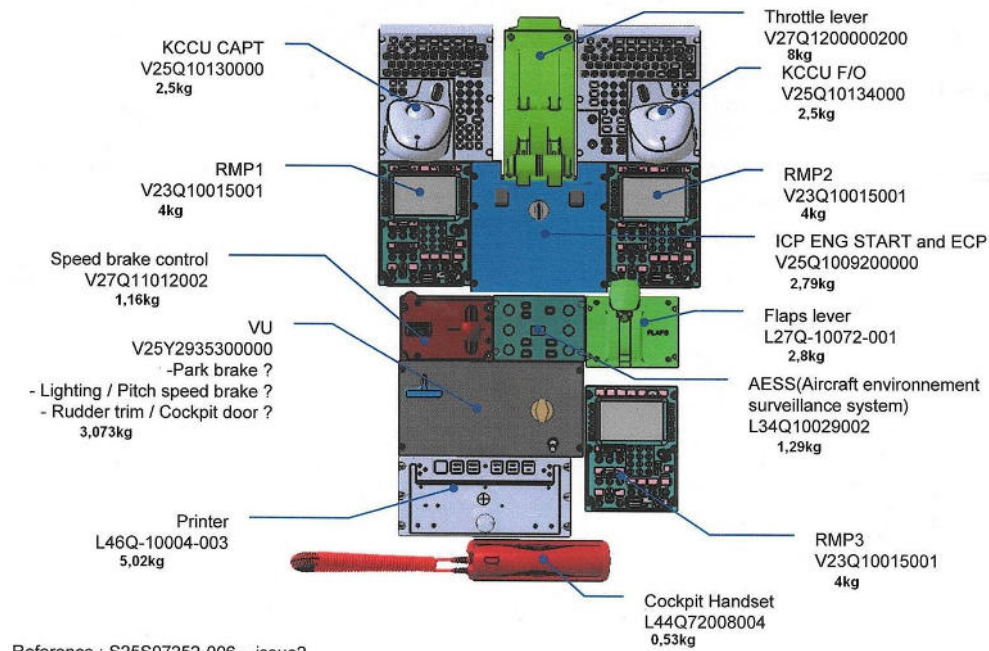
To save time the advantage of the symmetry is taken for the main structure and the canvas. Once the modelling of one side is finished, the grid can be reflected.

Non structural mass (NSM) is the fraction between the weight difference of the CAD- and the FE-model and the surface. The unit is $[\frac{kg}{mm^2}]$ which is consistently distributed on surface. PATRAN as well as CATIA can display the mass and the surface of a selected structure. The metallic frame has been reduced more than the remaining structure, so these two sections were

treated separately. The calculated mass per cubic millimeter is entered into the properties, PCOMP and PSHELL.

3.1.4 Export

The finite element analysis shall be performed with the program NASTRAN. Therefore it has to be exported the way that NASTRAN is capable to read the data. With "analyse" "model only" the mesh is written in a text document where every node location with its identification number (ID) is listed, every element number with its belonging nodes and property.



Reference : S25S07252-006 – issue2

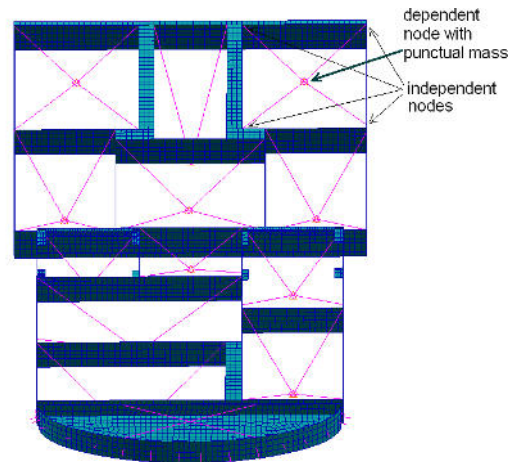


Figure 3.9: The electrical devices represented by 0D elements and connected with RBE3 elements

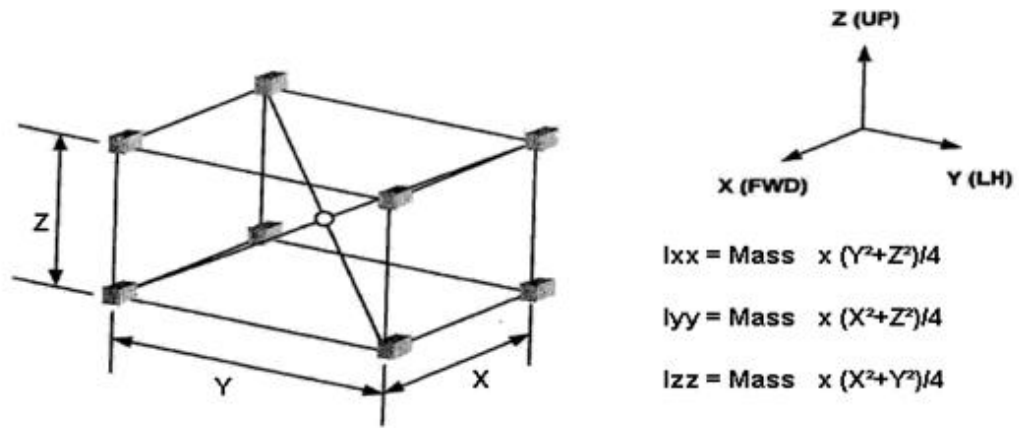


Figure 3.10: Calculation of the inertias of every electronic device

Laminated Composite				
Stacking Sequence Convention				Offset
Total ▼				-6.35
Stacking Sequence Definition				
	Material Name	Thickness	Orientation	
1	1000002	1.150000E-001	0.000000E+000	
2	1000002	1.150000E-001	9.000000E+001	
3	1000002	1.150000E-001	0.000000E+000	
4	1000002	1.150000E-001	9.000000E+001	
5	1000001	1.178000E+001	0.000000E+000	
6	1000002	1.150000E-001	9.000000E+001	
7	1000002	1.150000E-001	0.000000E+000	
8	1000002	1.150000E-001	9.000000E+001	
9	1000002	1.150000E-001	0.000000E+000	

Figure 3.11: The properties of sandwich structure with PATRAN

3.2 Modal analysis

3.2.1 Theory

The tendency of a system to oscillate at larger amplitude at some frequencies than at others is defined as resonance. These frequencies are known as the systems resonant frequencies. At these frequencies, even small periodic driving forces can produce large amplitude vibrations, because the system stores vibrational energy. By minimal damping, the resonant frequency is approximately equal to the natural frequency of the system, which is the frequency of free vibrations, the frequency at which a system naturally vibrates once it has been set into motion. In other words, the natural frequency is the number of times a system will oscillate (move back and forth) between its original position and its displaced position in a given time, if there is no outside interference.

A modal analysis is the study of the dynamic properties of structures under vibrational excitation. Modal analysis is the field of measuring and analysing the dynamic response of a structure when excited by an input. It is common to use the finite element method (FEM) to perform this analysis because, like other calculations using the FEM, the object being analyzed can have an arbitrary shape and the results of the calculations are acceptable. The types of equations which arise from modal analysis are those seen in eigensystems. The physical interpretation of the eigenvalues and eigenvectors which come from solving the system are that they represent the frequencies and corresponding mode shapes. In this case the only desired mode is the lowest frequency.

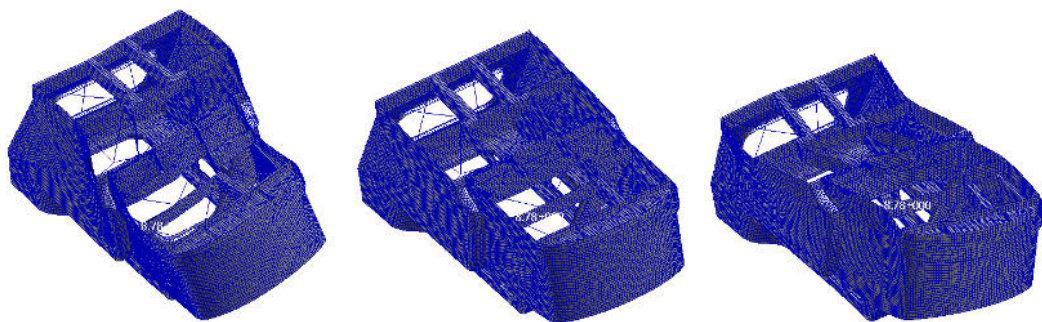


Figure 3.12: Displacements under natural frequency represented by animated deformation.

To assure that the structure will not be damaged during an aircraft life it has

to be proved that no resonant frequency is lower than the highest frequency of excitation of the plane. The excitation is caused by the turbines and can vary during utilization. The A350 is a plane that will fly above the sea for which the law decides that the plane has to be capable to fly with just one turbine in case of failure of the other. If only one turbine works, the plane vibrates at frequencies up to 25 Hz. To be sure that the structure is reliable the first mode of resonant frequency must be above 26 Hz. After exporting the finite element model from PATRAN the solver MSC NASTRAN calculates the first nine natural frequencies based on this equation:

$$f = \frac{1}{2 \cdot \pi} \cdot \sqrt{\frac{[K]}{[M]}} \quad (3.2.1)$$

For the most basic problem involving a linear elastic material which obeys Hooke's Law, the matrix equations take the form of a dynamic three dimensional spring mass system. The generalized equation of motion is given as:

$$[M]\ddot{\vec{u}} + [C]\dot{\vec{u}} + [K]u = \vec{F}(t) \quad (3.2.2)$$

where $[M]$ is the mass matrix, $\ddot{\vec{u}}$ (acceleration) is the 2nd time derivative of the displacement \vec{u} , $\dot{\vec{u}}$ is the velocity, $[C]$ is a damping matrix, $[K]$ is the stiffness matrix, and $\vec{F}(t)$ is the force vector. To obtain the resonant frequencies and the modes of vibration an undamped ($[C] = 0$), free oscillation ($\vec{F}(t) = 0$) is assumed.

The equation becomes:

$$[M]\ddot{\vec{u}} + [K]u = [0] \quad (3.2.3)$$

This is the general form of the eigensystem encountered in structural engineering using the FEM. \vec{u} is a harmonic oscillation:

displacement:

$$\vec{u} = \vec{A} \cos(\omega t) \quad (3.2.4a)$$

velocity:

$$\dot{\vec{u}} = -\omega \cdot \vec{A} \sin(\omega t) \quad (3.2.4b)$$

acceleration:

$$\begin{aligned}\vec{u} &= -\omega^2 \cdot \vec{A} \cos(\omega t) \\ &= -\omega^2 \cdot \vec{u}\end{aligned}\tag{3.2.4c}$$

Substituting equation 3.2.4 into equation 3.2.3 gives equation 3.2.5:

$$([K] - \omega^2[M]) \cdot \vec{u} = 0\tag{3.2.5}$$

The resonant frequency f can be calculated with

$$\omega = 2\pi \cdot f\tag{3.2.6}$$

and results in

$$f = \frac{\omega}{2\pi} = \frac{1}{2\pi} \cdot \sqrt{\frac{[K]}{[M]}}\tag{3.2.7}$$

The Amplitude \vec{u} from equation 3.2.5 can only be unequal zero if:

$$\det |[K] - \omega^2[M]| = 0\tag{3.2.8}$$

The values for ω^2 that make the term zero are called eigenvalues. By putting these eigenvalues into equation 3.2.7 the resonant frequencies can be found.

Once the finite element model of the centre pedestal was correctly determined a first calculation estimated a natural frequency of about 16Hz.

[Wik03b] [TM04] [SUD04] [Ste07] [WS06] [Raa06]

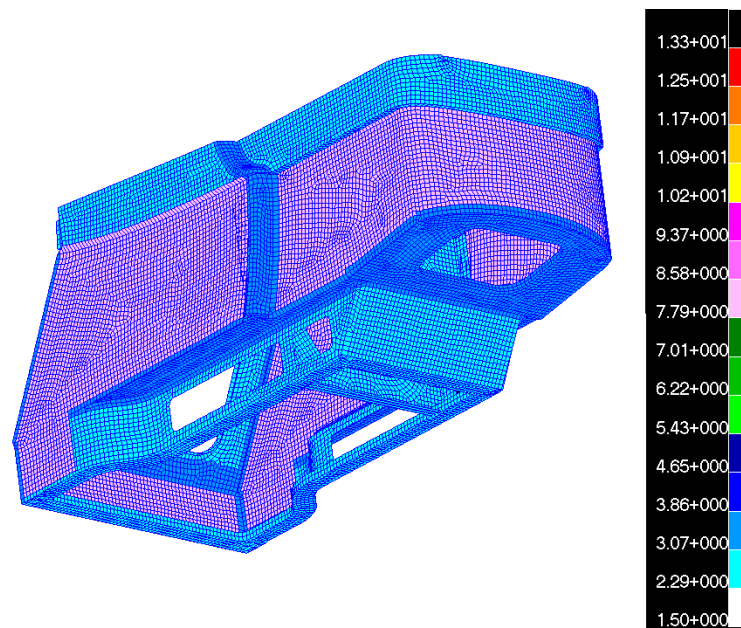


Figure 3.13: Completed FEM model before optimization. Thickness is represented by colour. Light blue: 12 layer of fibre glass preprag; Dark blue: 16 layer of fibre glass preprag; Pink: sandwich structure

3.2.2 Optimization

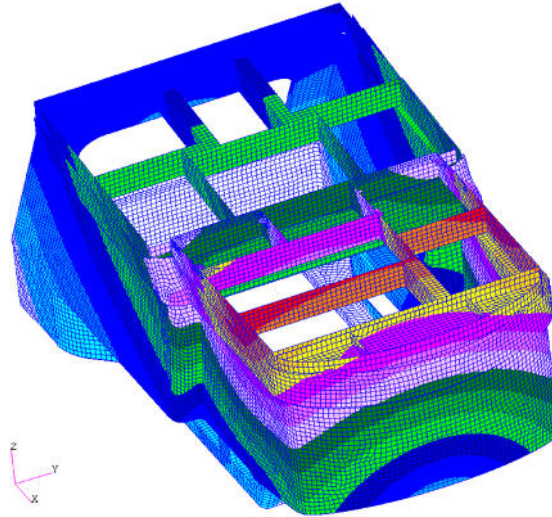


Figure 3.14: Displacements under first natural frequency of 26.3 Hz represented by colour. Red represents the largest displacement

The aim is to optimize the finite element model so that the first mode is above 26 Hz without passing 13.5 kg in structural mass. The structural mass is the weight of the centre pedestal without the weight of electrical devices. By looking at equation 3.2.1 above, it is obvious that the frequency f can be increased by increasing the rigidity K or by decreasing the mass M . The process of optimization proceeds as follows: The first objective is to increase the stiffness of the structure so that the first resonant frequency is higher than 26 Hz, proving, that it is generally possible to obtain such a lowest resonant frequency. Once the 26 Hz are achieved, the second objective is to decrease the mass without decreasing the actual natural frequency. The given materials are aluminium 2024 for the metallic frame, sandwich structure and either 12 or 16 layer of fibre reinforced preprags. Where modifications are made to increase stiffness or reduce weight, just these materials are used for simplicity. If some stuctures are shown to contain 24 layers in the calculation, it is simply twice the 12 layer. This does not complicate the manufacturing and keeps the cost low. To know what effects on weight and natural frequency a modification has, every modified model has to be calculated with NASTRAN and analysed wih PATRAN. Each calculation in normal modes takes about 30 minutes.

Stiffness increase

With PATRAN as post processor you have the possibility to visualize the deformation of the structure under oscillation of the resonant frequencies. It is possible to view the deformation at any time of one oscillation period between zero and 2π . A very helpful feature is "animate". "Animate" strings together the different deformations in a way that they become a movement which repeats over and over. A picture of an animation is shown on figure 3.12. This feature assists the comprehension of how the structure behaves under vibrations. Every antinode is visible and the swinging form is much clearer than in a coloured picture (see figure 3.14).

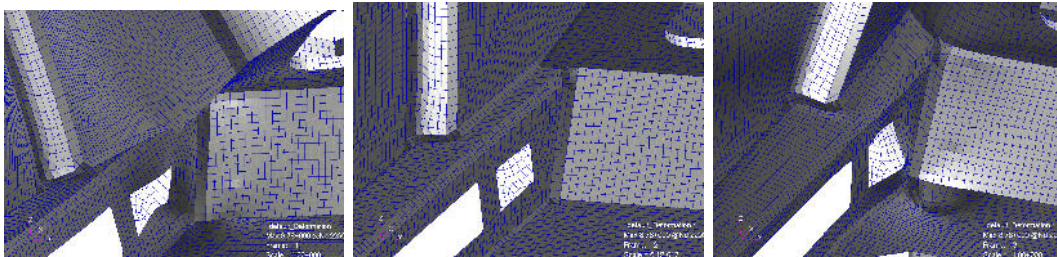


Figure 3.15: Critical zone

Model₀₁ - thicken front corners By observing the movement it is important to see where the biggest antinodes are and how they can be reduced. Figures 3.12 and 3.14 show that under first mode the upper part of the structure makes the biggest displacements. On the lower part of the structure, where the fixings are, is the least displacement. However, this is the essential part since it is the lower part that allows the upper part to move. Thus, to increase the natural frequency the rigidity of the centre pedestal's lower part should be increased. Figure 3.15 right shows a distortion where the fixing is, so this area could be stiffened by adding additional layer of fiber glass preprags. Furthermore the structure around the lower front window shows likewise a distortion. This area could be stiffened too. Another outstanding area is the jut above the windows. There, an additional support structure in form of a vertical triangle would reduce the buckling. But with the intention to change the design as little as possible on the viewable outer side, this area is just thickened (see figure 3.16). To get a first idea of the consequences thickening this area, the number of layers is doubled to 24 layers.

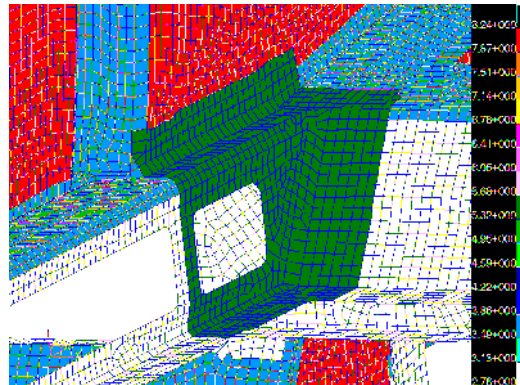


Figure 3.16: Rigidity increasement by adding several layer

The changes affect an increasement in natural frequency of 4.025 Hz, from 16.102 Hz to 20.127 Hz. After these changes the critical zone behaves the same but with smaller amplitudes.

Model₀₂ - window support structure Another effort to reduce the buckle near the window (see figure 3.15 rigth) is to harden the zone by adding a support structure around the windows (see figure 3.17). This configuration increased the fundamental frequency of 0.189 Hz from 16.102 Hz to 16.291 Hz.

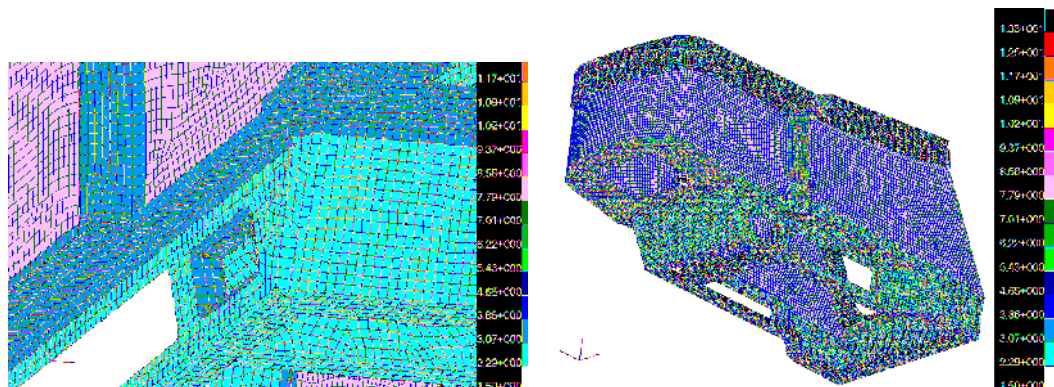


Figure 3.17: Left: *Modification₀₂* - adding a window support structure; Right: *Model₀₄* - thicken bottom part

Model₀₃ - **thicken canvas** Now that the front is more rigid, the biggest movements of the upper structure changed from the front more in the middle in x direction (see figure 3.18). That means that the canvas has to support more stress which is provoked by the swinging mass of the electrical devices. As result of this cognition the number of ply of the canvas increased from 12 to 16. On the unmodified model this change brought an increase of 0.169 Hz up to 16.271 Hz but on the *model₀₁* the natural frequency increased of 0.412 Hz from 20.127 Hz to 20.539 Hz.

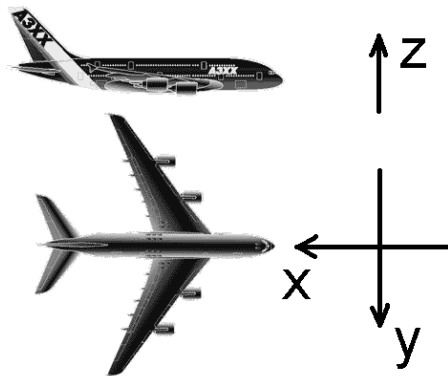


Figure 3.18: The origin of the coordinate system of an aircraft is on the tip of its nose

Model₀₄ - **thicken bottom part** The frequency increase of *Model₀₃* is not enough. To be more effective the whole bottom structure is updated to 24 ply of fibre glass preprags (see figure 3.17). This modification added 1.270 Hz compared to *Model₀₃* and resulted in a natural frequency of 21.809 Hz. Still not sufficient.

Model₀₅ - **thicken side parts** The main structure without metallic frame and canvas reminds a bit of a hull of a ship. Usually hulls were reinforced by semicircle ribs (see figure 3.19). These ribs function as stiffeners. By adding layer of fibre glass preprags the way figure 3.19 shows, this construction principle is imitated. The green elements arranged vertically on figure 3.19 have a thickness of 24 preprags and represent the stiffeners. This imitation permits to augment f of 2.289 Hz compared to *Model₀₄*. The fundamental frequency is 24.098 Hz.

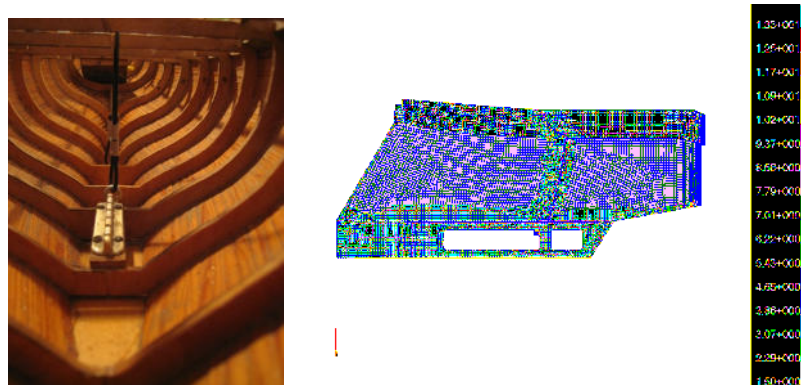


Figure 3.19: Left: Semicircle ribs in the hull of a ship that function as stiffeners;
Right: *Model*₀₅: Imitation of the construction of a hull

*Model*₀₆ - **additional fixings as an option** One option could be to add two fixings on the floor (see figure 3.21). Two more fixings would reduce the movement of the lower part which implies the reduction of the movement of the upper part. This modification has to be authorised by Airbus. Therefore, it could be a solution but should be avoided if possible. Anyhow, it is an option and by checking it, it brought an increase of 2.624 Hz compared to *Model*₀₅ and shows a fundamental frequency of 26.722 Hz. The fixings were placed on the area with the biggest oscillation (see figure 3.20).

With this modification the objective to reach 26 Hz is achieved. Now it is proven that it is possible to reach such a natural frequency. This leads to the next step, the mass reduction.

Mass reduction

*Model*₀₅ and *Model*₀₆ are models with 34208 Nodes and 31895 Elements. The whole centre pedestal (included electronical devices) weighs 57.153 kg. The mass of the electronical devices is 41.663 kg so the structure weighs 15.490 kg which means that 1.990 kg have to be reduced. And at the same time the natural frequency has to be above 26 Hz.

*Model*₀₇ - **new bottom structure** The "animate" mode shows that even with the changing on *Model*₀₄, by thickening the bottom part, it is still too

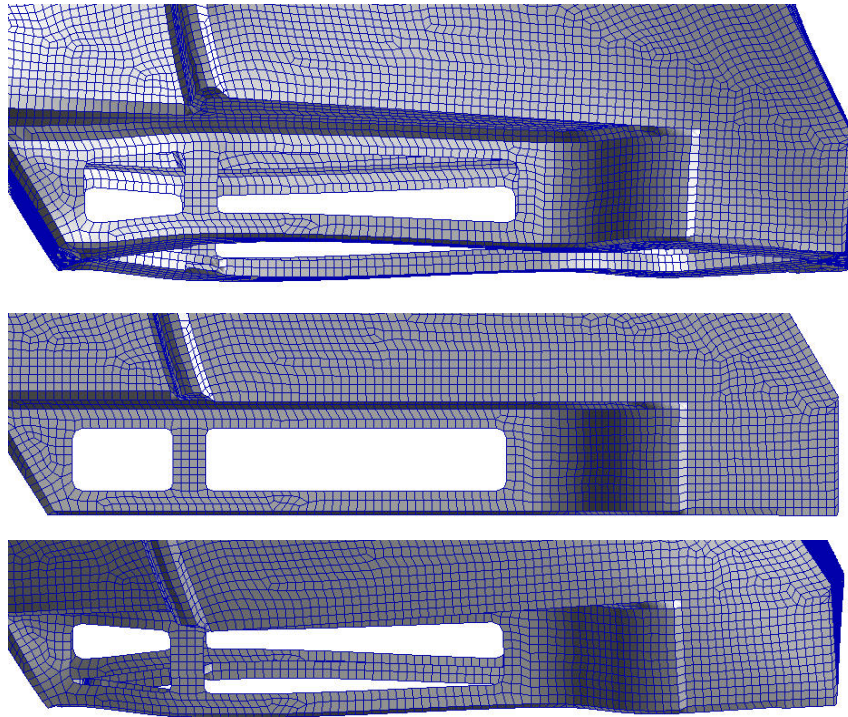


Figure 3.20: Movement under first natural frequency; Top: $-\pi$; Centre: 0; Down: π

flexible. Especially the structure under the long windows (see figure 3.20) shows a remarkable deformation. The biggest deformation is on the horizontal plane of the canvas. Between this plane and the front edges is no great distance so perhaps if they were connected together by a plane surface, the movements could be reduced that way, instead of adding two fixings. The same could be done from the other side but to keep the weight low, structure was only added near the corners (see figure 3.21 right). This enables embedding two continuous longitudinal stiffeners in x direction. Also in y direction are two stiffeners, so all around the new rectangular hole in the bottom surface are stiffeners. 90° corners can buckle easier than rounded edges. But instead of creating rounded edges, each corner is replaced by two 45° edges. This brings nearly the same effect and is faster to create under PATRAN.

With 25.513 Hz the natural frequency of *Model*₀₇ is 1.415 Hz higher than *Model*₀₅. The weight of its structure is 16.030 kg.

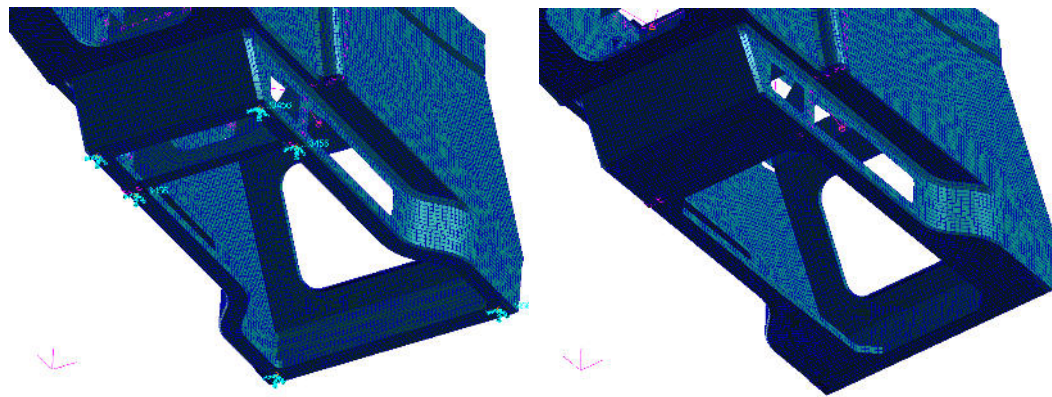


Figure 3.21: Left: *Model₀₆* - two additional fixings; Right: *Model₀₇* - new bottom surface

Model₀₈ - **thickness reduction** To reduce weight, thickness is reduced all over the bottom part around the critical zone, the vertical side parts and the corners because these are zones where local stiffness is essential for global stiffness. By this modification the fundamental frequency fell from 25.513 Hz to 25.258 Hz but also the weight fell by 840 g.

Model₀₉ - **skew bevel surface** Another change is that the rectangular skew bevel surface between the two edges is replaced by sandwich structure which has a lower density. This saves 90 gramms and increases the natural frequency by 0,065 Hz.

Model₁₀ - **adaption of structure** Sandwich can also be applied on other areas. Fixings in sandwich panels are possible but fixings in pure fibre glass preprags are easier to install. The front side and parts of the side structure are replaced by sandwich panels. Other areas are reduced in thickness, e.g. the bottom part of the bow, the side parts and the metallic frame. The canvas was reinforced on the areas where the main stress is seen. The borders are reinforced by additional plys and the upper border around the metallic frame is reduced in height. All these changes lead to a model that has a natural frequency of 26,363 Hz and a structural weight of 13,53 kg

The optimization ends here because the objectives are achieved.

3.3 Static analyses

To assure that the created model is also capable of supporting all different static load cases given by Airbus (see figure 3.22), the model is checked for all 42 load cases. The load cases are accelerations in different directions which the structure must resist to.

	Case name	INERTIAL load / LIMIT factor			INERTIAL load / Ultimate factor		
		X (g)	Y (g)	Z (g)	X (g)	Y (g)	Z (g)
Flight & Ground	Ft & Grd 1 (Fwd)	2,53	0,00	1,00	3,80	0,00	1,50
	Ft & Grd 2 (Rwd)	-1,82	0,00	1,00	-2,73	0,00	1,50
	Ft & Grd 3 (Left)	0,00	1,33	1,00	0,00	2,00	1,50
	Ft & Grd 4 (Right)	0,00	-1,33	1,00	0,00	-2,00	1,50
	Ft & Grd 5 (Dwn)	0,00	0,00	7,37	0,00	0,00	11,06
	Ft & Grd 6 (Up)	0,00	0,00	-3,68	0,00	0,00	-5,52
CRASH	Crash (Fwd)				9,00	0,00	0,00
	Crash (Rwd)				-3,00	0,00	0,00
	Crash (Left)				0,00	3,00	0,00
	Crash (Right)				0,00	-3,00	0,00
	Crash (Dwn)				0,00	0,00	6,00
	Crash (Up)				0,00	0,00	-3,00
SEI	SEI (Fwd)	1,21	0,00	0,00	1,89	0,00	0,00
	SEI (Rwd)	-1,21	0,00	0,00	-1,86	0,00	0,00
	SEI (Left)	0,00	1,21	0,00	0,00	2,14	0,00
	SEI (Right)	0,00	-1,21	0,00	0,00	-2,14	0,00
	SEI (Dwn)	0,00	0,00	2,21	0,00	0,00	3,86
	SEI (Up)	0,00	0,00	-0,21	0,00	0,00	-2,39
NWI	NWI (Fwd)	1,03	0,00	0,00	2,44	0,00	0,00
	NWI (Rwd)	-1,03	0,00	0,00	-2,44	0,00	0,00
	NWI (Left)	0,00	1,82	0,00	0,00	3,00	0,00
	NWI (Right)	0,00	-1,82	0,00	0,00	-3,00	0,00
	NWI (Dwn)	0,00	0,00	2,80	0,00	0,00	5,06
	NWI (Up)	0,00	0,00	-0,80	0,00	0,00	-2,06

Figure 3.22: Static loads prediction from Airbus

There are three kinds of checks that have to be done. The metallic frame has to be checked with the von Mises equation, the fibre glass preprags have to be checked with the Hill criterion and the shear stresses in the honeycomb layer have to be checked, too.

3.3.1 Von Mises

The metallic frame is checked by the Von Mises analysis. The verification of all load cases prove that the metallic frame resists to all load cases. Figure 3.23 shows the stresses of the "Flight & Ground - Down" load case. The scale on the left side indicates that the maximum stress is about 38.6 MPa. The $\sigma_{allowable}$ of aluminium is more than 400 MPa so there is no risk of breakage.

MSC.Patran 2006 r1a.06–Nov–09 15:07:15

Fringe: FG-UL_DOWN, Static Subcase, Stress Tensor, , von Mises, Minimum, 2 of 50 layers

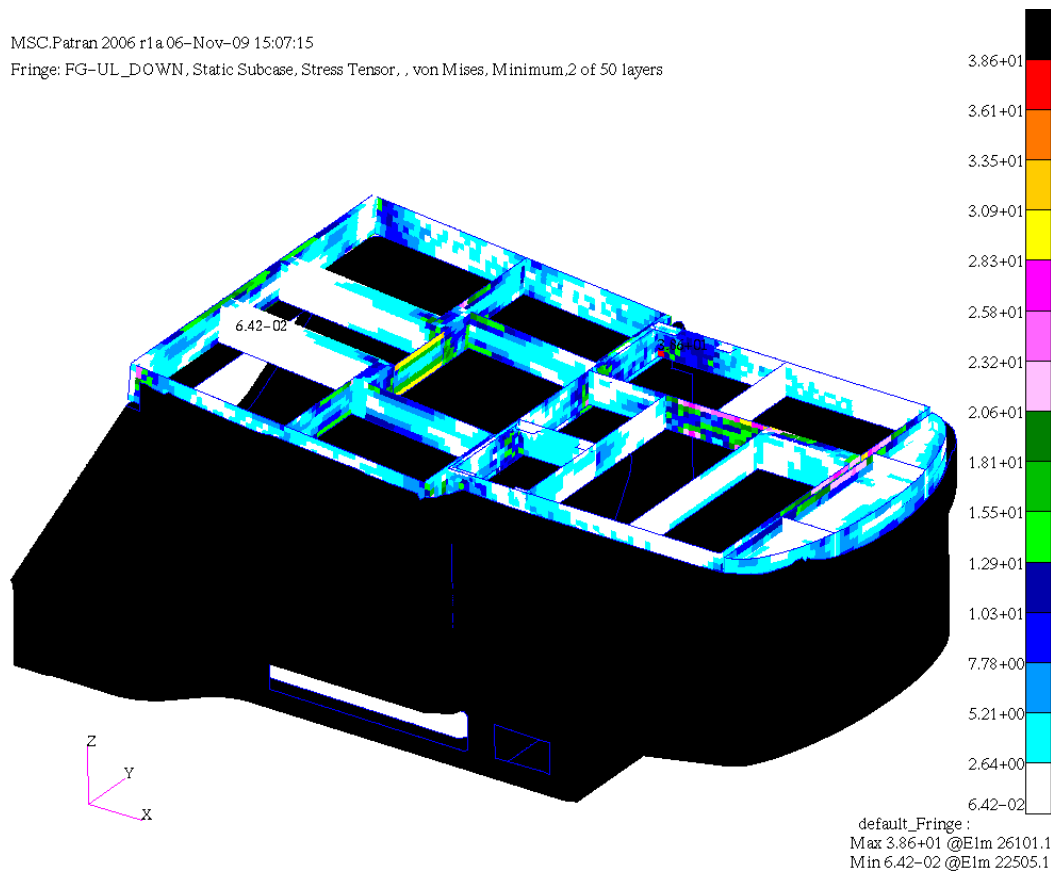


Figure 3.23: Von Mises verification on the metallic frame

By checking the composite with the Von Mises analysis, it turns out that the maximum stress is 164 MPa on the "FG-UL Down" load case where the structure has to support 11.06 times its own weight (see figure 3.24). So there is no risk for that because the composite materials can support at least 350 MPa in compression (and 355 MPa in tension). But the shear stresses have to be checked, too. This is done with the Hill criterion.

3.3.2 Hill criterion

The Hill criterion verifies all the ply that composes a PCOMP composite material. The Hill criterion considers interaction between the failure strengths.

The failure index is calculated as followed:

$$FailureIndex = h^2 = \left(\frac{\sigma_l}{R_l}\right)^2 + \left(\frac{\sigma_t}{R_t}\right)^2 + \left(\frac{\tau_{lt}}{S}\right)^2 - \frac{\sigma_l \cdot \sigma_t}{(R_l)^2} \quad (3.3.9)$$

Where:

- R_l is the longitudinal strength of the unidirectional layer in tension if $\sigma_l = 0$, in compression if $\sigma_l < 0$ (also in the $\sigma_l \cdot \sigma_t$ term),
- R_t is the transversal strength of the unidirectional layer in tension if $\sigma_t = 0$, in compression if $\sigma_t < 0$,
- S is the shear strength of the unidirectional layer.

Failure occurs if $h^2 = 1$. Considering a laminate composed of n layers, for each layer k ($k = 1$ to n) the Reserve Factor is :

$$RF_k = \frac{1}{\sqrt{h^2}} \quad (3.3.10)$$

The laminate overall Reserve Factor is the minimum of all Reserve Factors:

$$RF = \min(RF_k) \quad (3.3.11)$$

Figure 3.25 shows the RF on every element. If the RF value is less than 1, the structure breaks. On figure 3.25 top, only the elements where the fixings are, have a value less than 1. This is indicated by white colour. These elements can be ignored because the finite element methods do wrong calculations around fixings.

So there is no risk of preprag damage for the "Flight and Ground-UL-Reward" load case. But the "Flight and Ground-UL-Down" load case (see figure 3.25) shows white areas on other places than where the fixings are. This indicates that the material will break at this area.

3.3.3 Honeycomb YZ-, ZX-Components

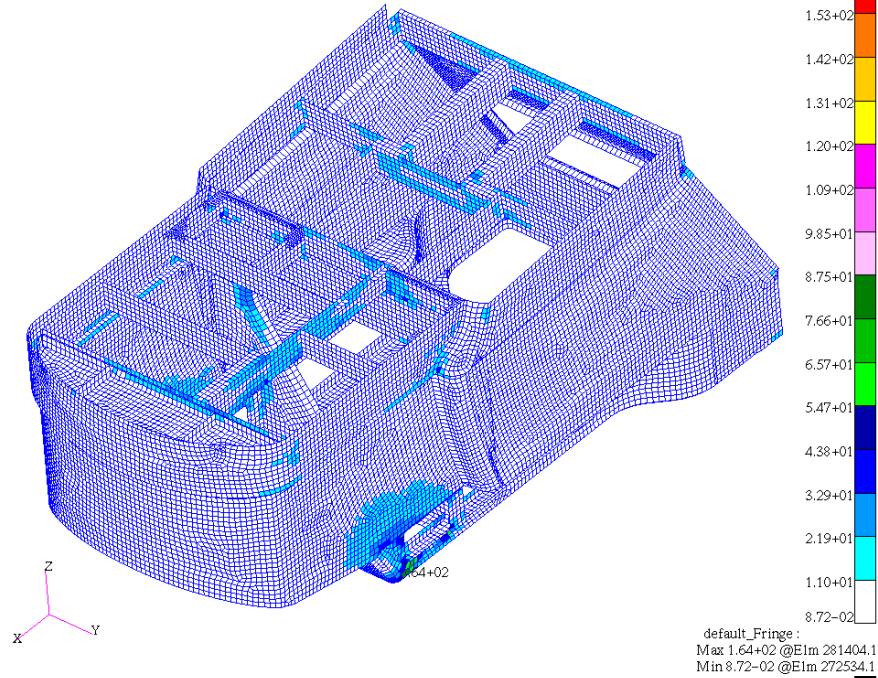
The honeycomb of the sandwich structure has to be verified apart (see figure 3.26). The honeycomb supports more stress in l-direction (0.75 MPa) than in w-direction (0.45 MPa). So if the maximum stress is between 0.45 MPa and 0.75 MPa, the material orientation has to be considered. This is not the case here. The maximum shear stress for the honeycomb is 0.31 MPa for the "FG-UL-Down" load case.

3.4 Conclusion

The centre pedestal has been optimized in natural frequency and weight. This optimization stopped once the objectives of 26 Hz and 13.5 kg have been reached. There are still possibilities of further optimization for example by changing more areas into sandwich structure. The verification of the Hill criterion shows that not all load cases are supported by the structure. Figure 3.25 shows on the lower screenshot where these areas are (white elements). These areas can be reinforced by additional layer(s) which would increase the weight of the structure and thus a further optimization in weight would be needed without decreasing the natural frequency. Even a lower value than 13.5 kg in structural weight is possible by applying more engineering work on the structure. Considering the fact that the status of the A350 is still MAT B, the results are satisfying. Also it is almost proved that a centre pedestal can be made of composite material instead of aluminium which is another step forward.

MSC.Patran 2006 r1a13--Aug-09 12:00:29

Fringe: FG-UL_DOWN, Static Subcase, Stress Tensor, , von Mises, Maximum,50 of 50 layers



MSC.Patran 2006 r1a13--Aug-09 12:00:29

Fringe: FG-UL_DOWN, Static Subcase, Stress Tensor, , von Mises, Maximum,50 of 50 layers

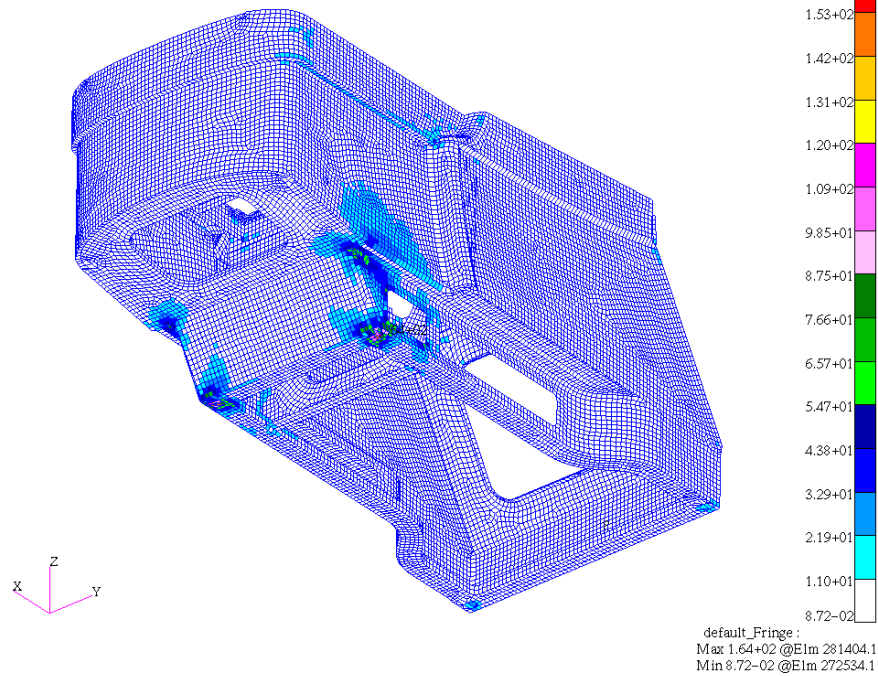
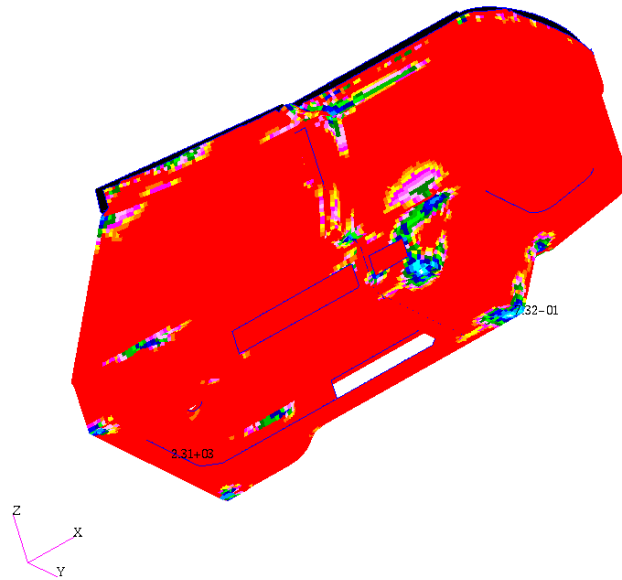


Figure 3.24: Von Mises verification on composite structure

MSC.Patran 2006 r1a.06-Nov-09 14:39:14

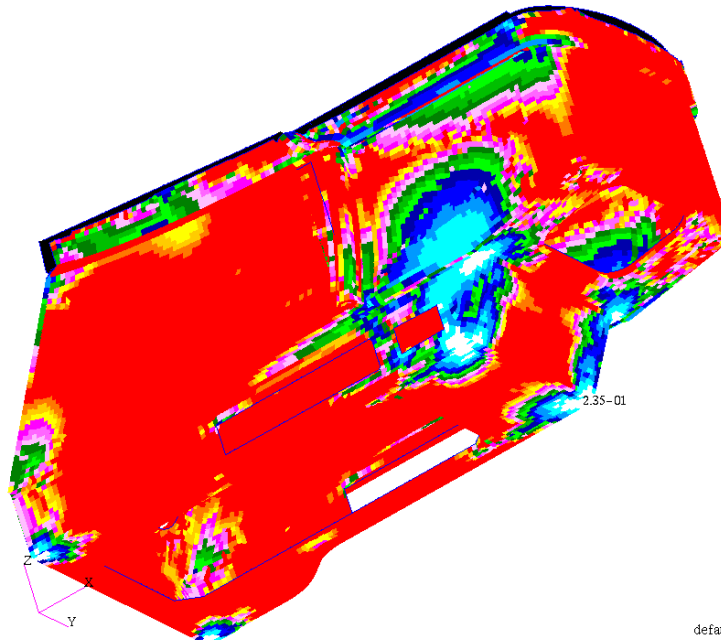
Fringe: FG-UL_RWD, Static Subcase, Criterion of Hill, Reserve Factor, , Minimum.48 of 48 layers



default_Fringe :
Max 2.31+03 @Elm 285769.1
Min 7.32-01 @Elm 281404.1

MSC.Patran 2006 r1a.06-Nov-09 15:03:00

Fringe: FG-UL_DOWN, Static Subcase, Criterion of Hill, Reserve Factor, , Minimum.48 of 48 layers



default_Fringe :
Max 1.04+03 @Elm 277515.1
Min 2.35-01 @Elm 281404.1

Figure 3.25: RF check: Top: the structure resists to the "FG-UL-Rwd" load case. Down: white elements are supposed to crack in the "FG-UL-Down"

List of Figures

1.1	ST GROUP logo	8
1.2	ST GROUP premises	8
1.3	The A400M MSN001 under construction [Mil09]	12
1.4	Bamboo structure	13
1.5	Left: Caulis of a plant. Right: Bamboo under microscope. The fibres are orientated like in fibre-reinforced composite. [Sch07]	14
1.6	Different types of composites. [Hex09]	15
1.7	Composites provide the advantages of lower weight, greater strength and higher stiffness. [Hex09]	16
1.8	Different preprag processing methods [Hex09]	18
1.9	Different sandwich cores [Wie07]	19
1.10	Sandwich compared to tissue composite [Hex09]	19
1.11	E_{\parallel} of a mixed layer of resin and uniaxial fibreglass	20
1.12	E_{\perp} of a mixed layer of resin and uniaxial fibreglass	21
1.13	$G_{\perp\parallel}$ of a mixed layer of resin and uniaxial fibreglass	21
1.14	$\nu_{\perp\parallel}$ of a mixed layer of resin and uniaxial fibreglass	22
1.15	Equivalence of forces	25
1.16	Equivalence of rigidity	25
1.17	PATRAN surface under UNIX	27
2.1	A400M cockpit furniture	29
2.2	The assembling of A400M cockpit furniture is done by sticking together the mortises and tenons in the production hall of ST Composites. The red circles signify two examples of the position of joints on the furniture. [ST3]	30
2.3	Sample dimensions	30
2.4	Tested joint types	31
2.5	Different Load Cases; Left: tension; Centre: compression; Right: shearing	32
2.6	Joint allowables provided by AIRBUS	32
2.7	Test results	33
2.8	Sandwich material	34

2.9	Left: The Eight Harness Satin pattern of the glass fibre tissue; Right: The honeycomb structure	35
2.10	Mortises and tenons stucked together and fixed with Henkel Hysol adhesive	36
2.11	Potting inserted in honeycomb	37
2.12	Finite element model of the L sample	38
2.13	Sandwich properties with PATRAN	38
2.14	Finite element model with 2D elements. X-axis in mm; Y-axis in N	39
2.15	Damage on the L sample after compressive loading	40
2.16	Top: RF distribution on L sample; Left: RF under tension; Right: RF under compression	41
2.17	Deflection of the mortise sandwich panel of the L sample under compressive load	46
2.18	Left: Sandwich flexion under moment load; centre: The dis- tributed displacement; right: The distributed stress	47
2.19	Delamination of the lower skin of L sample	47
2.20	The distribution of the shear stress	49
2.21	The distribution of the shear stress	50
2.22	The zigzag breaking line of a L sample under compression	52
3.1	Left: A350 cockpit preview [Fli09]; Right: ST3D center pedestal CAD model	55
3.2	The original given thickness	56
3.3	Metallic frame under CATIA V5	57
3.4	Left: CAD midplane surface model by using the symmetry; Right: Fixations	58
3.5	left: Volume structure; right: Midplane structure	58
3.6	Errors in the "paver" option; Left: Centre pedestal during mesh creation; Right: Zoom on the red square of the left figure show- ing too small elements	60
3.7	Zoom on the red square of figure 3.6 right showing a thin gap. .	61
3.8	RBE elements on the finite element model	62
3.9	The electrical devices represented by 0D elements and connected with RBE3 elements	66
3.10	Calculation of the inertias of every electronic device	67
3.11	The properties of sandwich structure with PATRAN	67
3.12	Displacements under natural frequency represented by animated deformation.	68

3.13	Completed FEM model before optimization. Thickness is represented by colour. Light blue: 12 layer of fibre glass preprag; Dark blue: 16 layer of fibre glass preprag; Pink: sandwich structure	71
3.14	Displacements under first natural frequency of 26.3 Hz represented by colour. Red represents the largest displacement	72
3.15	Critical zone	73
3.16	Rigidity increasement by adding several layer	74
3.17	Left: <i>Modification</i> ₀₂ - adding a window support structure; Right: <i>Model</i> ₀₄ - thicken bottom part	74
3.18	The origin of the coordinate system of an aircraft is on the tip of its nose	75
3.19	Left: Semicircle ribs in the hull of a ship that function as stiffeners; Right: <i>Model</i> ₀₅ : Imitation of the construction of a hull . .	76
3.20	Movement under first natural frequency; Top: $-\pi$; Centre: 0; Down: π	77
3.21	Left: <i>Model</i> ₀₆ - two additional fixings; Right: <i>Model</i> ₀₇ - new bottom surface	78
3.22	Static loads prediction from Airbus	79
3.23	Von Mises verification on the metallic frame	80
3.24	Von Mises verification on composite structure	83
3.25	RF check: Top: the structure resists to the "FG-UL-Rwd" load case. Down: white elements are supposed to crack in the "FG-UL-Down"	84
3.26	Verification of the shear stress inside the honeycomb (values in MPa)	85
.27	The A400M MSN001 on roll out [Mil09]	92
.28	AIRBUS A350 micro cutaway [mf09]	97

List of Tables

2.1	Fibreglass tissue material data	34
2.2	Honeycomb material data	35
2.3	Adhesive material data	36
2.4	Potting material data	37
2.5	The calculated results compared with the AIRBUS allowables and the test results in $[N/mm]$	51

Bibliography

- [Fli08] Flickr: *Bali - J.H. showroom*, 2008. <http://www.flickr.com/photos/suvajack/2192280512/in/photostream/>
- [Fli09] Flightglobal: *Cockpit*, 2009. <http://www.flightglobal.com/blogs/flight-international/Cockpit.gif>
- [Gay97] Gay, Daniel: *Matériaux composites*. Hermès, 1997, ISBN 2-86601-586-X.
- [Gro09] Group, ST: *Website*, 2009. <http://www.stgroup.aero>, visité le 22 juillet 2009.
- [Hex09] Hexcel: *Prepragtechnology.pdf*, 2009. <http://www.hexcel.com11/10/09>.
- [KE06] Kress, Gerald und Paolo Ermanni: *Mechanik der Faserverbundwerkstoffe*. Eidgenössische Technische Hochschule Zürich, 2006.
- [mf09] forum md80: *Website*, 2009. <http://www.md80.it/bbforum/viewtopic.php>, visited on 12/09/09.
- [Mil09] Military, Airbus: *Website*, 2009. <http://www.airbusmilitary.com>, visited on 11/10/09.
- [Raa06] Raatschen, Prof Dr H. J.: *Finite Elemente 1*. Fachhochschule Aachen, Fachbereich Maschinenbau, 2006.
- [Sch07] Schürmann, Helmut: *Konstruieren mit Faser-Kunststoff-Verbunden*. Springer-Verlag, 2007, ISBN 978-3-540-72189-5.
- [ST3] ST3D, rue du Bolé, 31673 Labège cedex: *company*. www.stgroup.aero.

- [Ste07] Steinke, Peter: *Finite-Elemente-Methode*. Springer Verlag, 2007, ISBN 978-3-540-72235-9.
- [SUD04] SUDRE, Michael: *Mécanique Vibratoire*. Université Paul Sabatier, GMP, 2004.
- [TM04] Tipler, Paul A. und Gene Mosca: *Physik*. Elsevier Spektrum akademischer Verlag, 2004, ISBN 3-8274-1164-5.
- [Wie07] Wiedemann, Johannes: *Leichtbau - Elemente und Konstruktion*. Springer-Verlag, 2007, ISBN 978-3-540-33656-7.
- [Wik01] Wikipedia: *Toulouse*, 01. <http://en.wikipedia.org/wiki/Toulouse>, visited on 22/07/09.
- [Wik02] Wikipedia: *Airbus a350*, 02. http://en.wikipedia.org/wiki/Airbus_A350, visited on 23/07/09.
- [Wik03a] Wikipedia: *Airbus a400m*, 03. <http://en.wikipedia.org/wiki/A400M>, visited on 23/07/09.
- [Wik03b] Wikipedia: *Modal analysis using fem*, 03. http://en.wikipedia.org/wiki/Modal_analysis_using_FEM, visited on 09/10/09.
- [Wik04] Wikipedia: *Composite material*, 04. http://en.wikipedia.org/wiki/Composite_material, visited on 23/07/09.
- [WS06] Wissmann, Johannes und Klaus Dieter Sarnes: *Finite Elemente in der Strukturmechanik*. Springer Verlag, 2006, ISBN 3-540-61836-8.

A400M



Figure .27: The A400M MSN001 on roll out [Mil09]

"The Airbus A400M is a European four-engine turboprop military transport aircraft that can be configured for aerial refueling. It has been designed by Airbus Military corporation to replace a variety of aircraft, including the Lockheed Martin C-130 Hercules and the Transall C-160. The A400M has been ordered by nine nations. [...]

The first test flight, originally scheduled for Q1 2008, was postponed due to program delays, schedule adjustments and financial pressures. EADS announced in early January 2008 that continued development problems with the engines had resulted in a delay to Q2 2008 before the first engine test flights on a C-130 testbed aircraft. The first flight of the aircraft, previously scheduled for July 2008, had again been postponed. Civil certification under EASA CS-25 will be followed later by certification for military purposes. The A400M was "rolled out" in Seville on 26 June 2008 at an event presided by King Juan Carlos I of Spain, while the maiden flight is now facing on-going technical delays and is unlikely to happen earlier than late 2009. [...]

The Airbus A400M will increase the airlift capacity and range compared with the aircraft it was originally set to replace, the older versions of the Hercules and Transall. Cargo capacity is expected to double over existing aircraft, both in payload and volume, and range is increased substantially as well. The cargo

box dimensions are: Length, excluding ramp 17.71 m; ramp length 5.40 m; width 4.00 m; height 3.85 m; height, aft of wing 4.00 m.

The Airbus A400M will operate in many configurations including cargo transport, troop transport, MEDEVAC, aerial refuelling, and electronic surveillance.

The cockpit features a fly-by-wire flight control system with sidestick controllers and flight envelope protection. Like Airbus' other aircraft, the A400M will have a full glass cockpit (all information accessed through large colour screens) and as such will represent a technological leap compared to the older C-130s and C-160s that many countries now operate.

The A400M's wings are primarily carbon fibre reinforced plastic. The eight-bladed Scimitar propeller is also made from a woven composite material. It is powered by four Europrop TP400-D6 rated at 8,250 kW (11,000 hp) each.

EADS and Thales will provide the new Multi-Color Infrared Alerting Sensor (MIRAS) missile warning sensor for the A400M.

General characteristics

- Crew: 3 or 4 (2 pilots, 3rd optional, 1 loadmaster)
- Capacity:
 - 37,000 kg (82,000 lb)
 - 116 fully equipped troops / paratroops,
 - up to 66 stretchers accompanied by 25 medical personnel
- Length: 43.8 m (143 ft 8 in)
- Wingspan: 42.4 m (139 ft 1 in)
- Height: 14.6 m (47 ft 11 in)
- Empty weight: 70 tonnes (154,000 lb)

- Max takeoff weight: 141 tonnes (310,852 lb)
- Powerplant: 4x EuroProp International TP400-D6 turboprop, 8,250 kW (11,000 hp) each
- Total Internal Fuel: 46.7 tonnes (103,000 lb)
- Max. Landing Weight: 114 tonnes (251,000 lb)

Performance

- Cruise speed: 780 km/h (420 kt, 485 mph Mach 0.68 - 0.72)
- Initial Cruise Altitude: at MTOW: 9,000 m (29,000 ft))
- Range: 3,300 km (1,782 nmi) at max payload (long range cruise speed; reserves as per MIL-C-5011A)
 - Range at 30-tonne payload: 4,800 km (2,592 nmi)
 - Range at 20-tonne payload: 6,950 km (3,753 nmi)
- Ferry range: 9,300 km (5,022 nmi)
- Service ceiling: 11,300 m (37,000 ft) Maximum Operating Altitude: 12,000 m (40,000 ft)
- Tactical Takeoff Distance: 940 m (3,080 ft) (aircraft weight 100 tonnes, soft field, ISA, sea level)
- Tactical Landing Distance: 625 m (2,050 ft) (as above)
- Turning Radius (Ground): 28.6 m "

[Wik03a]

A350

"The Airbus A350 XWB (Xtra Wide-Body) is a long range, mid-sized, wide-body family of airliners currently under development by European manufacturing group Airbus. The A350 will be the first Airbus with fuselage and wing structures made primarily of carbon fibre reinforced plastic. The A350 is designed to compete with the Boeing 777 and the Boeing 787 and Airbus claims that it will be more fuel-efficient and with up to 8% lower operating cost than the Boeing 787. It is scheduled to enter into airline service in 2013. The Launch Customer for the Airbus A350 will be Qatar Airways. [...]

When Boeing announced its 787 Dreamliner project, it claimed the lower operating costs of this airplane would make it a serious threat to the Airbus A330. Publicly, Airbus initially rejected this claim, stating that the 787 was itself just a reaction to the A330, and that no response was needed to the 787.

The airlines pushed Airbus to provide a competitor, as Boeing had committed the 787 to have 20% lower fuel consumption than the Boeing 767. Initially Airbus proposed a simple derivative of the A330, unofficially dubbed the 'A330-200Lite', with improved aerodynamics and engines similar to those on the 787. The airlines were not satisfied and Airbus committed €4 billion to a new design to be called the A350. The original version of the A350 superficially resembled the A330 due to its common fuselage cross-section and assembly. A new wing, engines and a horizontal stabilizer were to be coupled with new composite materials and production methods applied to the fuselage to make the A350 an almost all-new aircraft. [...]

In September 2007, Airbus rolled out new design advances to a gathering of 100 representatives from existing and potential XWB customers. The A350 XWB will be built on the technologies developed for Airbus A380 and will have a similar cockpit and fly-by-wire systems layout. The A350XWB will be made out of 53% composites, 19% Al/Al-Li, 14% titanium, 6% steel and 8% miscellaneous. This compares to the Boeing 787, which consists of 50% composites, 20% aluminium, 15% titanium, 10% steel and 5% the balance. October 2008 was the Airbus internal goal to freeze the design and Airbus expects 10% lower airframe maintenance cost and 14% lower empty seat weight than competing aircraft.

There are three variants of the A350 and all launched in 2006. The A350-900 is scheduled to enter service in 2013. The A350-800 is scheduled to enter service in 2014. The A350-1000 is scheduled to enter service in 2015. All variants will

be offered as corporate jets by wholly-owned subsidiary Airbus Executive and Private Aviation.

A350-800

The A350-800 will seat 270 passengers in a three-class cabin nine-abreast layout and will have a range of 8,300 nmi (15,400 km). It is designed to compete with the Boeing 787-9 and to directly replace the Airbus A330-200.

A350-900

The A350-900 is the first model scheduled to enter service (EIS) in 2013 and seats 314 passengers in a three-class cabin nine-abreast layout. It will have a range of 8,100 nmi (15,000 km). Airbus claim that the A350-900 will have a decrease of 16% MWE per seat, a 30% decrease in block fuel per seat and 25% better cash operating cost against the Boeing 777-200ER. A -900R and -900F variant also is being proposed but not launched yet and will feature the higher engine thrust, strengthened structure and landing gear of the -1000. It is designed to compete with the Boeing 777-200ER and replace the A340-300.

A350-1000

The A350-1000 is scheduled to enter service in 2015. It is the largest variant of the A350 family and will seat 350 passengers in a three-class cabin nine-abreast layout. It will have range of 8,000 nmi (14,800 km). It is designed to compete with the Boeing 777-300ER and replace the A340-600.

As of July 2009, 31 customers have placed 493 firm orders for the A350XWB." [Wik02]

Figure .28 shows the A350 as micro cutaway.



97

MAT1

Isotropic Material Property Definition

Defines the material properties for linear isotropic materials.

Format:

1	2	3	4	5	6	7	8	9	10
MAT1	MID	E	G	NU	RHO	A	TREF	GE	
	ST	SC	SS	MCSID					

Example:

MAT1	17	3.+7		0.33	4.28	6.5-6	5.37+2	0.23	
	20.+4	15.+4	12.+4	1003					

Field	Contents
MID	Material identification number. (Integer > 0)
E	Young’s modulus. (Real ≥ 0.0 or blank)
G	Shear modulus. (Real ≥ 0.0 or blank)
NU	Poisson’s ratio. (-1.0 < Real ≤ 0.5 or blank)
RHO	Mass density. See Remark 5. (Real)
A	Thermal expansion coefficient. (Real)
TREF	Reference temperature for the calculation of thermal loads, or a temperature-dependent thermal expansion coefficient. See Remarks 9. and 10. (Real; Default = 0.0 if A is specified.)
GE	Structural element damping coefficient. See Remarks 8., 9., and 4. (Real)
ST, SC, SS	Stress limits for tension, compression, and shear are optionally supplied, used only to compute margins of safety in certain elements; and have no effect on the computational procedures. See “Parameters” on page 1409. (Real ≥ 0.0 or blank)
MCSID	Material coordinate system identification number. Used only for PARAM,CURV processing. See “Parameters” on page 1409. (Integer ≥ 0 or blank)

MAT8

Shell Element Orthotropic Material Property Definition

Defines the material property for an orthotropic material for isoparametric shell elements.

Format:

1	2	3	4	5	6	7	8	9	10
MAT8	MID	E1	E2	NU12	G12	G1Z	G2Z	RHO	
	A1	A2	TREF	Xt	Xc	Yt	Yc	S	
	GE	F12	STRN						

Example:

MAT8	171	30.+6	1.+6	0.3	2.+6	3.+6	1.5+6	0.056	
	28.-6	1.5-6	155.0	1.+4	1.5+4	2.+2	8.+2	1.+3	
	1.-4		1.0						

Field	Contents
MID	Material identification number. Referenced on a PSHELL or PCOMP entry only. (0 < Integer < 1000000000)
E1	Modulus of elasticity in longitudinal direction, also defined as the fiber direction or 1-direction. (Real ≠ 0.0)
E2	Modulus of elasticity in lateral direction, also defined as the matrix direction or 2-direction. (Real ≠ 0.0)
NU12	Poisson’s ratio (ϵ_2 / ϵ_1 for uniaxial loading in 1-direction). Note that $\nu_{21} = \epsilon_1 / \epsilon_2$ for uniaxial loading in 2-direction is related to ν_{12} , E_1 , and E_2 by the relation $\nu_{12}E_2 = \nu_{21}E_1$. (Real)
G12	In-plane shear modulus. (Real ≥ 0.0; Default = 0.0)
G1Z	Transverse shear modulus for shear in 1-Z plane. (Real > 0.0; Default implies infinite shear modulus.)
G2Z	Transverse shear modulus for shear in 2-Z plane. (Real > 0.0; Default implies infinite shear modulus.)
RHO	Mass density. (Real)
Ai	Thermal expansion coefficient in i-direction. (Real)

Field	Contents
TREF	Reference temperature for the calculation of thermal loads, or a temperature-dependent thermal expansion coefficient. See Remarks 4. and 5. (Real or blank)
Xt, Xc	Allowable stresses or strains in tension and compression, respectively, in the longitudinal direction. Required if failure index is desired. See the FT field on the PCOMP entry. (Real > 0.0; Default value for Xc is Xt.)
Yt, Yc	Allowable stresses or strains in tension and compression, respectively, in the lateral direction. Required if failure index is desired. (Real > 0.0; Default value for Yc is Yt.)
S	Allowable stress or strain for in-plane shear. See the FT field on the PCOMP entry. (Real > 0.0)
GE	Structural damping coefficient. See Remarks 4. and 6. (Real)
F12	Interaction term in the tensor polynomial theory of Tsai-Wu. Required if failure index by Tsai-Wu theory is desired and if value of F12 is different from 0.0. See the FT field on the PCOMP entry. (Real)
STRN	For the maximum strain theory only (see STRN in PCOMP entry). Indicates whether Xt, Xc, Yt, Yc, and S are stress or strain allowables. [Real = 1.0 for strain allowables; blank (Default) for stress allowables.]

Remarks:

1. If G1Z and G2Z values are specified as zero or blank, then transverse shear flexibility calculations will not be performed, which is equivalent to zero shear flexibility (i.e., infinite shear stiffness).
2. An approximate value for G1Z and G2Z is the in-plane shear modulus G12. If test data are not available to accurately determine G1Z and G2Z for the material and transverse shear calculations are deemed essential; the value of G12 may be supplied for G1Z and G2Z. In SOL 106, linear and nonlinear elastic material properties in the residual structure will be updated as prescribed in the TEMPERATURE Case Control command.
3. Xt, Yt, and S are required for composite element failure calculations when requested in the FT field of the PCOMP entry. Xc and Yc are also used but not required.
4. TREF and GE are ignored if this entry is referenced by a PCOMP entry.
5. TREF is used in two different ways:

CONM2 Concentrated Mass Element Connection, Rigid Body Form

Defines a concentrated mass at a grid point.

Format:

1	2	3	4	5	6	7	8	9	10
CONM2	EID	G	CID	M	X1	X2	X3		
	I11	I21	I22	I31	I32	I33			

Example:

CONM2	2	15	6	49.7					
	16.2		16.2			7.8			

Field	Contents
EID	Element identification number. (Integer > 0)
G	Grid point identification number. (Integer > 0)
CID	Coordinate system identification number. For CID of -1; see X1, X2, X3 below. (Integer \geq -1; Default = 0)
M	Mass value. (Real)
X1, X2, X3	Offset distances from the grid point to the center of gravity of the mass in the coordinate system defined in field 4, unless CID = -1, in which case X1, X2, X3 are the coordinates, not offsets, of the center of gravity of the mass in the basic coordinate system. (Real)
Iij	Mass moments of inertia measured at the mass center of gravity in the coordinate system defined by field 4. If CID = -1, the basic coordinate system is implied. (For I11, I22, and I33; Real \geq 0.0; for I21, I31, and I32; Real)

Remarks:

1. Element identification numbers should be unique with respect to all other element identification numbers.
2. For a more general means of defining concentrated mass at grid points, see the CONM1 entry description.
3. The continuation is optional.

CQUAD4

Quadrilateral Plate Element Connection

Defines an isoparametric membrane-bending or plane strain quadrilateral plate element.

Format:

1	2	3	4	5	6	7	8	9	10
CQUAD4	EID	PID	G1	G2	G3	G4	THETA or MCID	ZOFFS	
			T1	T2	T3	T4			

Example:

CQUAD4	111	203	31	74	75	32	2.6	0.3	
			1.77	2.04	2.09	1.80			

Field	Contents
EID	Element identification number. (Integer > 0)
PID	Property identification number of a PSHELL, PCOMP, or PLPLANE entry. (Integer > 0; Default = EID)
Gi	Grid point identification numbers of connection points. (Integers > 0, all unique.)
THETA	Material property orientation angle in degrees. THETA is ignored for hyperelastic elements. See Figure 5-43 . (Real; Default = 0.0)
MCID	Material coordinate system identification number. The x-axis of the material coordinate system is determined by projecting the x-axis of the MCID coordinate system (defined by the CORDij entry or zero for the basic coordinate system) onto the surface of the element. MCID is ignored for hyperelastic elements. (Integer ≥ 0; If blank, then THETA = 0.0 is assumed.)

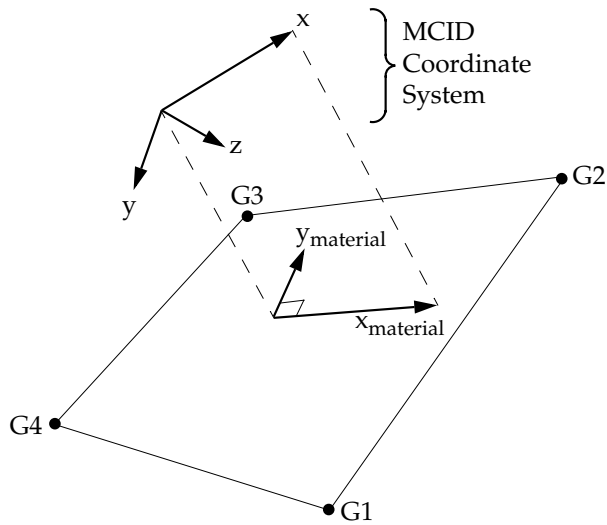


Figure 5-42 MCID Coordinate System Definition

ZOFFS	Offset from the surface of grid points to the element reference plane. ZOFFS is ignored for hyperelastic elements. See Remark 6. (Real)
Ti	Membrane thickness of element at grid points G1 through G4. Ti are ignored for hyperelastic elements. (Real ≥ 0.0 or blank, not all zero. See Remark 4. for default.)

Remarks:

1. Element identification numbers should be unique with respect to all other element identification numbers.
2. Grid points G1 through G4 must be ordered consecutively around the perimeter of the element.
3. All interior angles must be less than 180° .
4. The continuation is optional. If it is not supplied, then T1 through T4 will be set equal to the value of T on the PSHELL entry.

CTRIA3

Triangular Plate Element Connection

Defines an isoparametric membrane-bending or plane strain triangular plate element.

Format:

1	2	3	4	5	6	7	8	9	10
CTRIA3	EID	PID	G1	G2	G3	THETA or MCID	ZOFFS		
			T1	T2	T3				

Example:

CTRIA3	111	203	31	74	75	3.0	0.98		
			1.77	2.04	2.09				

Field	Contents
EID	Element identification number. (Integer > 0)
PID	Property identification number of a PSHELL, PCOMP or PLPLANE entry. (Integer > 0; Default = EID)
Gi	Grid point identification numbers of connection points. (Integers>0, all unique)
THETA	Material property orientation angle in degrees. THETA is ignored for hyperelastic elements. (Real; Default = 0.0)
MCID	Material coordinate system identification number. The x-axis of the material coordinate system is determined by projecting the x-axis of the MCID coordinate system (defined by the CORDij entry or zero for the basic coordinate system) onto the surface of the element. MCID is ignored for hyperelastic elements. (Integer ≥ 0; if blank, then THETA = 0.0 is assumed.)

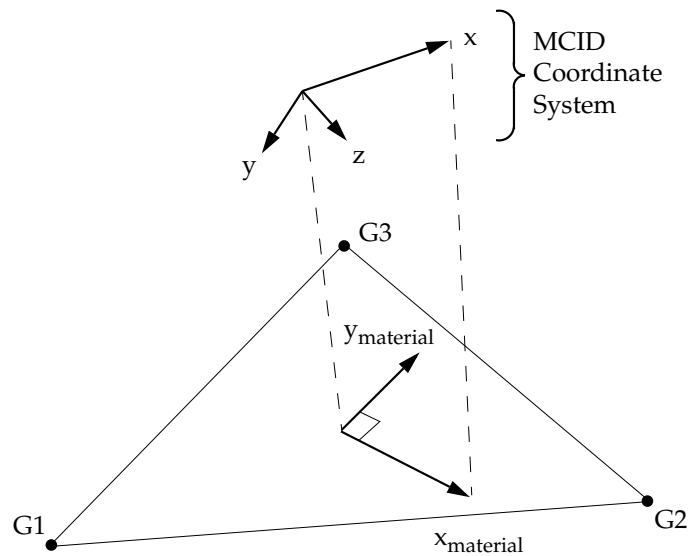


Figure 5-61 MCID Coordinate System Definition

ZOFFS	Offset from the surface of grid points to the element reference plane. See Remark 3. ZOFFS is ignored for hyperelastic elements. (Real)
Ti	Membrane thickness of element at grid points G1, G2, and G3. Ti is ignored for hyperelastic elements. (Real ≥ 0.0 or blank, not all zero. See Remark 2. for default.)

Remarks:

1. Element identification numbers should be unique with respect to all other element identification numbers.
2. The continuation is optional. If it is not supplied, then T1 through T3 will be set equal to the value of T on the PSHELL entry.
3. Elements may be offset from the connection points by means of the ZOFFS field. Other data, such as material matrices and stress fiber locations, are given relative to the reference plane. A positive value of ZOFFS implies that the element reference plane is offset a distance of ZOFFS along the positive Z-axis of the element coordinate system. If the ZOFFS field is used, then both the MID1 and MID2 fields must be specified on the PSHELL entry referenced by PID.

The specification of offset vectors gives wrong results in solution sequences that compute differential stiffness: linear buckling analysis provided in SOLs 5, 16, 105 and 200, and geometric nonlinear analysis provided in SOLs 106, 129, 153, and 159 with PARAM,LGDISP,1.

PCOMP

Layered Composite Element Property

Defines the properties of an n-ply composite material laminate.

Format:

1	2	3	4	5	6	7	8	9	10
PCOMP	PID	Z0	NSM	SB	FT	TREF	GE	LAM	
	MID1	T1	THETA1	SOUT1	MID2	T2	THETA2	SOUT2	
	MID3	T3	THETA3	SOUT3	-etc.-				

Example:

PCOMP	181	-0.224	7.45	10000.0	HOFF				
	171	0.056	0.	YES			45.		
			-45.				90.		

Field	Contents
PID	Property identification number. (0 < Integer < 10000000)
Z0	Distance from the reference plane to the bottom surface. See Remark 10. (Real; Default = -0.5 times the element thickness.)
NSM	Nonstructural mass per unit area. (Real)
SB	Allowable shear stress of the bonding material (allowable interlaminar shear stress). Required if FT is also specified. (Real > 0.0)
FT	Failure theory. The following theories are allowed (Character or blank. If blank, then no failure calculation will be performed): "HILL" for the Hill theory. "HOFF" for the Hoffman theory. "TSAI" for the Tsai-Wu theory. "STRN" for the Maximum Strain theory.
TREF	Reference temperature. See Remark 3. (Real; Default = 0.0)
GE	Damping coefficient. See Remarks 4. and 12. (Real; Default = 0.0)
LAM	Laminte Options. (Character or blank, Default = blank). See Remark 13. "Blank" All plies must be specified and all stiffness terms are developed.

Field	Contents
	<p>“SYM” Only plies on one side of the element centerline are specified. The plies are numbered starting with 1 for the bottom layer. If an odd number of plies are desired, the center ply thickness (T1 or TN) should be half the actual thickness.</p> <p>“MEM” All plies must be specified, but only membrane terms (MID1 on the derived PSHELL entry) are computed.</p> <p>“BEND” All plies must be specified, but only bending terms (MID2 on the derived PSHELL entry) are computed.</p>
MIDi	Material ID of the various plies. The plies are identified by serially numbering them from 1 at the bottom layer. The MIDi must refer to MAT1, MAT2, or MAT8 Bulk Data entries. See Remark 1. (Integer > 0 or blank, except MID1 must be specified.)
Ti	Thicknesses of the various plies. See Remark 1. (Real or blank, except T1 must be specified.)
THETAi	Orientation angle of the longitudinal direction of each ply with the material axis of the element. (If the material angle on the element connection entry is 0.0, the material axis and side 1-2 of the element coincide.) The plies are to be numbered serially starting with 1 at the bottom layer. The bottom layer is defined as the surface with the largest -Z value in the element coordinate system. (Real; Default = 0.0)
SOUTi	Stress or strain output request. See Remarks 5. and 6. (Character: “YES” or “NO”; Default = “NO”)

Remarks:

1. The default for MID2, ..., MIDn is the last defined MIDi. In the example above, MID1 is the default for MID2, MID3, and MID4. The same logic applies to Ti.
2. At least one of the four values (MIDi, Ti, THETAi, SOUTi) must be present for a ply to exist. The minimum number of plies is one.
3. The TREF specified on the material entries referenced by plies are not used. Instead TREF on the PCOMP entry is used for all plies of the element. If not specified, it defaults to “0.0.”

PSHELL Shell Element Property

Defines the membrane, bending, transverse shear, and coupling properties of thin shell elements.

Format:

1	2	3	4	5	6	7	8	9	10
PSHELL	PID	MID1	T	MID2	12I/T**3	MID3	TS/T	NSM	
	Z1	Z2	MID4						

Example:

PSHELL	203	204	1.90	205	1.2	206	0.8	6.32	
	+.95	-.95							

Field	Contents
PID	Property identification number. (Integer > 0)
MID1	Material identification number for the membrane. (Integer ≥ 0 or blank)
T	Default membrane thickness for Ti on the connection entry. If T is blank then the thickness must be specified for Ti on the CQUAD4, CTRIA3, CQUAD8, and CTRIA6 entries. (Real or blank)
MID2	Material identification number for bending. (Integer ≥ -1 or blank)
12I/T**3	Bending moment of inertia ratio, $12I/T^3$. Ratio of the actual bending moment inertia of the shell, I , to the bending moment of inertia of a homogeneous shell, $T^3/12$. The default value is for a homogeneous shell. (Real > 0.0; Default = 1.0)
MID3	Material identification number for transverse shear. (Integer > 0 or blank; unless MID2 > 0, must be blank.)
TS/T	Transverse shear thickness ratio, T_s/T . Ratio of the shear thickness, (T_s) , to the membrane thickness of the shell, T . The default value is for a homogeneous shell. (Real > 0.0; Default = .833333)
NSM	Nonstructural mass per unit area. (Real)

Z1, Z2	Fiber distances for stress calculations. The positive direction is determined by the right-hand rule, and the order in which the grid points are listed on the connection entry. See Remark 11. for defaults. (Real or blank)
MID4	Material identification number for membrane-bending coupling. See Remarks 6. and 13. (Integer > 0 or blank, must be blank unless MID1 > 0 and MID2 > 0, may not equal MID1 or MID2.)

Remarks:

1. All PSHELL property entries should have unique identification numbers with respect to all other property entries.
2. The structural mass is calculated from the density using the membrane thickness and membrane material properties.
3. The results of leaving an MID field blank (or MID2 = -1) are:

MID1	No membrane or coupling stiffness
MID2	No bending, coupling, or transverse shear stiffness
MID3	No transverse shear flexibility
MID4	No bending-membrane coupling unless ZOFFS is specified on the connection entry. See Remark 6.
MID2=-1	See Remark 12.

Note: MID1 and MID2 must be specified if the ZOFFS field is also specified on the connection entry.
4. The continuation entry is not required.
5. The structural damping (GE on the MATi entry) is obtained from MID1 material.
6. The following should be considered when using MID4.
 - The MID4 field should be left blank if the material properties are symmetric with respect to the middle surface of the shell. If the element centerline is offset from the plane of the grid points but the material properties are symmetric, the preferred method for modeling the offset is by use of the ZOFFS field on the connection entry. Although the MID4 field may be used for this purpose, it may produce ill-conditioned stiffness matrices (negative terms on factor diagonal) if done incorrectly.

RBE2 Rigid Body Element, Form 2

Defines a rigid body with independent degrees-of-freedom that are specified at a single grid point and with dependent degrees-of-freedom that are specified at an arbitrary number of grid points.

Format:

1	2	3	4	5	6	7	8	9	10
RBE2	EID	GN	CM	GM1	GM2	GM3	GM4	GM5	
	GM6	GM7	GM8	-etc.-					

Example:

RBE2	9	8	12	10	12	14	15	16	
	20								

Field	Contents
EID	Element identification number. (Integer > 0)
GN	Identification number of grid point to which all six independent degrees-of-freedom for the element are assigned. (Integer > 0)
CM	Component numbers of the dependent degrees-of-freedom in the global coordinate system at grid points GMi. (Integers 1 through 6 with no embedded blanks.)
GMi	Grid point identification numbers at which dependent degrees-of-freedom are assigned. (Integer > 0)

Remarks:

1. The components indicated by CM are made dependent (members of the m-set) at all grid points GMi.
2. Dependent degrees-of-freedom assigned by one rigid element may not also be assigned dependent by another rigid element or by a multipoint constraint.
3. Element identification numbers should be unique with respect to all other element identification numbers.
4. Rigid elements, unlike MPCs, are not selected through the Case Control Section.

RBE3 Interpolation Constraint Element

Defines the motion at a reference grid point as the weighted average of the motions at a set of other grid points.

Format:

1	2	3	4	5	6	7	8	9	10
RBE3	EID		REFGRID	REFC	WT1	C1	G1,1	G1,2	
	G1,3	WT2	C2	G2,1	G2,2	-etc.-	WT3	C3	
	G3,1	G3,2	-etc.-	WT4	C4	G4,1	G4,2	-etc.-	
	"UM"	GM1	CM1	GM2	CM2	GM3	CM3		
		GM4	CM4	GM5	CM5	-etc.-			

Example

RBE3	14		100	1234	1.0	123	1	3	
	5	4.7	1	2	4	6	5.2	2	
	7	8	9	5.1	1	15	16		
	UM	100	14	5	3	7	2		

Field	Contents
EID	Element identification number. Unique with respect to other rigid elements. (Integer > 0)
REFGRID	Reference grid point identification number. (Integer > 0)
REFC	Component numbers at the reference grid point. (Any of the Integers 1 through 6 with no embedded blanks.)
WTi	Weighting factor for components of motion on the following entry at grid points Gi,j. (Real)
Ci	Component numbers with weighting factor WTi at grid points Gi,j. (Any of the Integers 1 through 6 with no embedded blanks.)
Gi,j	Grid points with components Ci that have weighting factor WTi in the averaging equations. (Integer > 0)
"UM"	Indicates the start of the degrees-of-freedom belonging to the m-set. The default action is to assign only the components in REFC to the m-set. (Character)

Field	Contents
GMI	Identification numbers of grid points with degrees-of-freedom in the m-set. (Integer > 0)
CMi	Component numbers of GMI to be assigned to the m-set. (Any of the Integers 1 through 6 with no embedded blanks.)

Remarks:

1. It is recommended that for most applications only the translation components 123 be used for Ci. An exception is the case where the Gi,j are colinear. A rotation component may then be added to one grid point to stabilize its associated rigid body mode for the element.
2. Blank spaces may be left at the end of a Gi,j sequence.
3. The default for "UM" should be used except in cases where the user wishes to include some or all REFC components in displacement sets exclusive from the the m-set. If the default is not used for "UM":
 - The total number of components in the m-set (i.e., the total number of dependent degrees-of-freedom defined by the element) must be equal to the number of components in REFC (four components in the example).
 - The components specified after "UM" must be a subset of the components specified under REFC and (Gi,j, Ci).
 - The coefficient matrix $[R_m]$ described in Section 9.4.3 of the *MSC.Nastran Reference Manual* must be nonsingular. PARAM,CHECKOUT in SOLs 101 through 200 may be used to check for this condition.
4. Dependent degrees-of-freedom assigned by one rigid element may not also be assigned dependent by another rigid element or by a multipoint constraint.
5. Rigid elements, unlike MPCs, are not selected through the Case Control Section.
6. Forces of multipoint constraint may be recovered in all solution sequences, except SOL 129, with the MPCFORCE Case Control command.
7. Rigid elements are ignored in heat transfer problems.
8. The m-set coordinates specified on this entry may not be specified on other entries that define mutually exclusive sets. See "**Degree-of-Freedom Sets**" on page 1573 for a list of these entries.

SPC

Single-Point Constraint

Defines a set of single-point constraints and enforced motion (enforced displacements in static analysis and enforced displacements, velocities or acceleration in dynamic analysis).

Format:

1	2	3	4	5	6	7	8	9	10
SPC	SID	G1	C1	D1	G2	C2	D2		

Example:

SPC	2	32	3	-2.6	5				
-----	---	----	---	------	---	--	--	--	--

Field	Contents
SID	Identification number of the single-point constraint set. (Integer > 0)
Gi	Grid or scalar point identification number. (Integer > 0)
Ci	Component number. (0 ≤ Integer ≤ 6; up to six Unique Integers, 1 through 6, may be placed in the field with no embedded blanks. 0 applies to scalar points and 1 through 6 applies to grid points.)
Di	Value of enforced motion for all degrees-of-freedom designated by Gi and Ci. (Real)

Remarks:

- Single-point constraint sets must be selected with the Case Control command SPC = SID.
- Degrees-of-freedom specified on this entry form members of the mutually exclusive s-set. They may not be specified on other entries that define mutually exclusive sets. See “**Degree-of-Freedom Sets**” on page 1573 for a list of these entries.
- Single-point forces of constraint are recovered during stress data recovery.
- From 1 to 12 degrees-of-freedom may be specified on a single entry.
- Degrees-of-freedom on this entry may be redundantly specified as permanent constraints using the PS field on the GRID entry.
- For reasons of efficiency, the SPCD entry is the preferred method for applying enforced motion rather than the Di field described here.